THE EFFECT OF IMPERFECTIONS ON THE BUCKLING OF THIN WALLED CYLINDRICAL SHELLS

Thesis by

Robert L. Ditchey

In Partial Fulfillment of the Requirements

For the Degree of

Aeronautical Engineer

California Institute of Technology

Pasadena, California

1973

(Submitted May 25, 1973)

ACKNOWLEDGMENT

The author feels very sincerely that this work is but an incremental step in comparison to the accomplishments of many engineers and theoreticians who have studied this topic. The intellect and the dedication of so many inspires both awe and humility.

The author is deeply indebted to Dr. C. D. Babcock, Jr. for his guidance, patience, and encouragement during the course of this work, and to Dr. J. Arbocz for his generous assistance and understanding. In particular, a great debt is owed to Dr. E. E. Sechler, without whose assistance none of this would have been possible.

Gratitude is due to Elizabeth Fox for her great skill and the patience shown in typing this thesis, and to Betty Wood for preparing the figures.

Finally, a very special word of gratitude is expressed to the author's wife and children for their encouragement, patience, and the many sunny weekends spent at home.

ABSTRACT

A theoretical study of the effect of imperfections on the buckling load of a circular cylindrical shell under axial compression was carried out.

The nonlinear shell equations of Donnell are solved in an approximate manner using the Potential Energy Theorem. The method of derivation and the resulting algebraic equations are compared to previous derivations which use a different method of solution. It was found that the resulting equations are identical to the ones derived by Galerkin's procedure, lending credence to that method.

A parametric study of an imperfection model was carried out numerically. The imperfection model is similar to that originally used by Donnell, having amplitude decay with increasing wave number. The results show the effect of various rates of decay of amplitude with wave number, as well as the effect of various assumed amplitudes. Using these parameters, it is shown when shell buckling is dominated by long wave imperfections as opposed to classical short wave imperfections.

It was found that if the decay of asymmetric imperfections with axial wave number is sufficiently high, that long wave imperfections can dominate. In the range of values chosen for these parameters, changes in the axisymmetric imperfection model had little effect on buckling behavior as compared to the changes in sensitivity to long waves which occur as the asymmetric model is varied.

LIST OF SYMBOLS

A_1, A_2, A_3, etc.	coefficients given on page 29
B_1, B_2, B_3, etc.	coefficients given on page 29
a_1, a_2, a_3, etc.	coefficients given on page 30
b_1, b_2, b_3, etc.	coefficients given on page 30
c	$= \sqrt{3(1-\nu^2)}$
E	Young's modulus
G_1, G_2	operators defined on pages 5 and 6
i, k	axial half wave numbers
ℓ	circumferential wave numbers
L	length of shell
$M_1, M_2, M_3, M_6, M_9, M_9$	coefficients of N_y
N_1, N_5, N_6, N_8, N_9	coefficients of N_x
N_x, N_y, N_{xy}	Stress Resultants, defined on page 8
P_1, P_3, P_4	coefficients of N_{xy}
q	decay constant operating on i
r	decay constant operating on k
R	shell radius
s	decay constant operating on ℓ
t	shell thickness
U	Potential Energy
U_1, U_2, U_3	integrals representing contributions to the total potential energy

LIST OF SYMBOLS (Cont'd)

u, v	displacements
w	radial displacement, positive outward
$\overline{w}$	radial imperfection (displacement) from perfect circular cylinder
x, y	axial and circumferential coordinates on the middle surface of the shell, respectively
$\overline{X}_A, \overline{X}$	axisymmetric and asymmetric imperfection amplitude used in the imperfection models, respectively
$a_i, a_k, a_{i+k}, a_{i-k}, \beta, \overline{\gamma}_k, \overline{\gamma}_k, \overline{\gamma}_{i+k}, \overline{\gamma}_{i-k}$	mode shape parameters defined on page 34
$\epsilon_x, \epsilon_y, \gamma_{xy}$	strain, defined on page 8
ν	Poisson's Ratio
λ	nondimensional loading parameter = $\frac{Rc\sigma}{Et}$
σ	axial stress
ξ_i	nondimensional radial displacement amplitude
$\overline{\xi}_i$	nondimensional initial imperfection amplitude

LIST OF FIGURES

LIST OF TABLES

TABLE OF CONTENTS

TABLE OF CONTENTS (Cont'd)

I. GENERAL INTRODUCTION

The buckling load of isotropic thin-walled cylindrical shells under axial compression cannot be accurately predicted by linearized small deflection theory. Classical theory of this general category predicts a collapse load which is never reached in experimental work. Moreover, the results of numerous experiments indicate that a very complex phenomenon must be involved.

The general problem of cylinders in axial compression has been investigated and discussed by a very great number of authors. The reader is referred to Fung and Sechler (Ref. 1) for a detailed discussion and a listing of some of the many writings on this topic. For a discussion of the role of imperfections in shell buckling, the reader is referred to Arbocz and Babcock (Ref. 2).

The work presented herein represents an amplification of the theory presented by Arbocz and Babcock. In that paper the imperfect shell equations are solved in an approximate manner using a two mode deflection assumption and a Galerkin approach. The resulting algebraic equations are simplified by neglecting cubic terms in comparison to the quadratic terms (Ref. 3). The circumferential periodicity condition (Ref. 4) is not considered in the formulation.

A study of the influence of these assumptions on the resulting algebraic equations is one objective of this work. Figure 1 is a graphical display of the rationale involved.

Starting with the assumptions made in the derivation of the nonlinear shell equations of Donnell (Ref. 5) one may choose to use

a Galerkin type of approximation procedure, or to follow a potential energy method of formulation. Having chosen either of these paths, two branches then exist for each — whether to seek a particular solution to the compatibility equation (a stress function formulation) or to seek a particular solution to the inplane equilibrium equations (a displacement formulation). Variations in method then follow depending upon the specific way by which periodicity of the circumferential displacement is satisfied. Considering just the Galerkin procedure, different methods can be obtained depending upon variations in the weighting function. Considering the method of solving the inplane equilibrium equations, different methods may be obtained depending upon whether or not one allows for a constant term in the radial displacement. This term would permit a uniform expansion.

The Galerkin procedure used by Arbocz and Babcock (and others) left open the mathematical validity of the specific weighting function to be used — an essential and all-important factor in the analysis. Since it was recognized that the Galerkin procedure was approximate, it was desirable to derive a solution to the Donnell equations using a potential energy method and compare the results.

It should also be understood that an essential factor which will introduce variations in all methods is the mathematic model for radial displacement and the imperfections (modal decomposition). For example, the method followed herein is a two mode representation using cosine axial representation for a general axisymmetric term and sine axial representation for a general asymmetric term. One could, of course, introduce complexity by using more than two

modes and one could use a different trigonometric representation. It is clear from earlier work that a two mode solution does lead to numerical inaccuracy, as compared to using more than two modes, and that experimental measurements show significant prebuckling growth of more than two model components (Ref. 2). On the other hand, since it was an objective of this work to compare the end result of the Galerkin method used by Arbocz and Babcock with a potential energy derived solution, it was considered appropriate to use the simplest model for radial displacement which captures the essential nature of the physics, i.e., the two mode case. As will be described subsequently, the parametric study of sensitivity to imperfections also dictated simplicity from a computational time standpoint.

A second objective of this work was to carry out a numerical study of imperfection sensitivity using as a basis the data from a recent investigation conducted by Arbocz and Babcock (Ref. 6). This work, which uses an imperfection model introduced by Imbert (Ref. 7), clearly showed that proper modal decomposition of imperfections should include asymmetric components, and should include a decay of imperfection amplitudes with increasing wave numbers.

The numerical work presented in this paper is an expansion on this topic. Presented herein is a parametric study which shows the effect that various decay rates have on the buckling load, when buckling can be dominated by lower order modes, and how the various parameters of the imperfection models proposed in reference 6 are interrelated.

II. THEORETICAL FORMULATION

This section is devoted to the derivation of the appropriate algebraic equations which represent an approximate solution to the nonlinear Donnell equations. The approach taken is to solve the inplane equilibrium for the displacements u and v after an assumption is made on the radial displacement w and the initial imperfection $\bar{w}$. The third equilibrium equation is satisfied in an approximate manner using the Potential Energy Theorem.

1. Donnell Shell Equations

Using the nonlinear Donnell equations, the two inplane equilibrium equations for an isotropic cylindrical shell may be written (in terms of displacement) as:

$$\frac{\partial^2 u}{\partial x^2} + \frac{(1-\nu)}{2}\frac{\partial^2 u}{\partial y^2} + \frac{(1+\nu)}{2}\frac{\partial^2 v}{\partial x \partial y} = -G_1(w,\bar{w}) \tag{1}$$

$$\frac{\partial^2 v}{\partial y^2} + \frac{(1-\nu)}{2}\frac{\partial^2 v}{\partial x^2} + \frac{(1+\nu)}{2}\frac{\partial^2 u}{\partial x \partial y} = -G_2(w,\bar{w}) \tag{2}$$

where the operators $G_1(w,\bar{w})$ and $G_2(w,\bar{w})$ are given by:

$$\begin{aligned} G_1(w,\bar{w}) = {} & \frac{\partial^2 w}{\partial x^2}\cdot\frac{\partial(w+\bar{w})}{\partial x} + \frac{(1+\nu)}{2}\frac{\partial w}{\partial y}\cdot\frac{\partial^2(w+\bar{w})}{\partial x \partial y} \\ & + \frac{(1-\nu)}{2}\frac{\partial^2 w}{\partial y^2}\cdot\frac{\partial(w+\bar{w})}{\partial x} + \frac{\nu}{R}\frac{\partial w}{\partial x} + \\ & + \frac{\partial^2 w}{\partial x^2}\cdot\frac{\partial w}{\partial x} + \frac{(1+\nu)}{2}\frac{\partial \bar{w}}{\partial y}\cdot\frac{\partial^2 w}{\partial x \partial y} \\ & + \frac{(1-\nu)}{2}\frac{\partial^2 \bar{w}}{\partial y^2}\cdot\frac{\partial w}{\partial x} \end{aligned} \tag{3}$$

and

$$G_2(w,\bar{w}) = \frac{\partial^2 w}{\partial y^2} \cdot \frac{\partial(w+\bar{w})}{\partial y} + \frac{(1+\nu)}{2} \frac{\partial w}{\partial x} \cdot \frac{\partial^2(w+\bar{w})}{\partial x \partial y} +$$

$$+ \frac{(1-\nu)}{2} \frac{\partial^2 w}{\partial x^2} \cdot \frac{\partial(w+\bar{w})}{\partial y} + \frac{1}{R} \frac{\partial w}{\partial y} + \frac{\partial^2 \bar{w}}{\partial y^2} \cdot \frac{\partial w}{\partial y} +$$

$$+ \frac{(1+\nu)}{2} \frac{\partial \bar{w}}{\partial x} \cdot \frac{\partial^2 w}{\partial x \partial y} + \frac{(1-\nu)}{2} \frac{\partial^2 \bar{w}}{\partial x^2} \cdot \frac{\partial w}{\partial y} \qquad (4)$$

2. Mode Selection

Assuming the following representation for the displacement w and the imperfections $\bar{w}$:

$$w = \xi_1 t \cos i\pi \frac{x}{L} + \xi_2 t \sin k\pi \frac{x}{L} \cos \ell \frac{y}{R} + \xi_3 t \qquad (5)$$

$$\bar{w} = \bar{\xi}_1 t \cos i\pi \frac{x}{L} + \bar{\xi}_2 t \sin k\pi \frac{x}{L} \cos \ell \frac{y}{R} \qquad (6)$$

and performing the operations given by G_1 and G_2, the right hand side of equations (1) and (2) are given by:

$$G_1(w,\bar{w}) = A_1 \sin 2i\pi \frac{x}{L} + A_2 \sin i\pi \frac{x}{L} +$$

$$+ A_3 \sin 2k\pi \frac{x}{L} + A_4 \cos k\pi \frac{x}{L} \cos \ell \frac{y}{R} +$$

$$+ A_5 \sin 2k\pi \frac{x}{L} \cos 2\ell \frac{y}{R} +$$

$$+ A_6 \cos(i+k)\pi \frac{x}{L} \cos \ell \frac{y}{R} +$$

$$+ A_7 \cos(i-k)\pi \frac{x}{L} \cos \ell \frac{y}{R} \qquad (7)$$

$$G_2(w,\overline{w}) = B_1 \sin 2\ell \frac{y}{R} + B_2 \cos 2k\pi \frac{x}{L} \sin 2\ell \frac{y}{R} +$$

$$+ B_3 \sin(i+k)\pi \frac{x}{L} \sin \ell \frac{y}{R} +$$

$$+ B_4 \sin(i-k)\pi \frac{x}{L} \sin \ell \frac{y}{R} +$$

$$+ B_5 \sin k\pi \frac{x}{L} \sin \ell \frac{y}{R} \qquad (8)$$

where the coefficients A_i and B_i are given in Appendix I. A particular solution to the two inplane equilibrium equations is then obtained. It is assumed that the form of the displacements u and v are given by:

$$u_p = a_1 \sin 2i\pi \frac{x}{L} + a_2 \sin i\pi \frac{x}{L} +$$

$$+ a_3 \sin 2k\pi \frac{x}{L} + a_4 \cos k\pi \frac{x}{L} \cos \ell \frac{y}{R} +$$

$$+ a_5 \sin 2k\pi \frac{x}{L} \cos 2\ell \frac{y}{R} +$$

$$+ a_6 \cos(i+k)\pi \frac{x}{L} \cos \ell \frac{y}{R} +$$

$$+ a_7 \cos(i-k)\pi \frac{x}{L} \cos \ell \frac{y}{R} \qquad (9)$$

and

$$v_p = b_1 \sin 2\ell \frac{y}{R} + b_2 \cos 2k\pi \frac{x}{L} \sin 2\ell \frac{y}{R}$$

$$+ b_3 \sin(i+k)\pi \frac{x}{L} \sin \ell \frac{y}{R} +$$

$$+ b_4 \sin(i-k)\pi \frac{x}{L} \sin \ell \frac{y}{R} +$$

$$+ b_5 \sin k\pi \frac{x}{L} \sin \ell \frac{y}{R} \qquad (10)$$

Note that periodicity of the circumferential displacement is satisfied without the need of introducing a homogeneous solution as is necessary in a stress function approach (Ref. 4).

Differentiating u_p and v_p as given by the left hand side of equations (1) and (2), and equating coefficients of like trigonometric terms, algebraic equations which determine the coefficients of u_p and v_p are obtained, i. e., the coefficients a_i and b_i are determined in terms of the coefficients A_i and B_i. These coefficients are given in Appendix II.

3. Boundary Conditions

In order to satisfy the boundary conditions on the displacement u, one must find an appropriate homogeneous solution

$$u(x, y) = u_p(x, y) + u_o + u_1 x \tag{11}$$

The boundary condition at x = 0 is

$$u(0, y) = 0 \tag{12}$$

or

$$u_o = -u_p(0, y)$$

now

$$u_p(0, y) = a_4 \cos \ell \frac{y}{R} + a_6 \cos \ell \frac{y}{R} + a_7 \cos \ell \frac{y}{R}$$

The satisfaction of this boundary condition with the simplified homogeneous solution is not possible. However, an "average" type boundary condition, i. e.

$$\int_0^{2\pi R} [u_p(0, y) + u_o] \, dy = 0$$

can be satisfied and gives

$$u_o = 0$$

The stress resultant N_x at $x = L$ will be used to determine u_1.

4. Stress Resultants

Using the constitutive relations

$$N_x = \frac{Et}{1-\nu^2} (\epsilon_x + \nu \epsilon_y)$$

$$N_y = \frac{Et}{1-\nu^2} (\epsilon_y + \nu \epsilon_x)$$

$$N_{xy} = \frac{Et}{2(1+\nu)} \gamma_{xy} \tag{13}$$

and the strain-displacement relations

$$\epsilon_x = \frac{\partial u}{\partial x} + \frac{1}{2} \left(\frac{\partial w}{\partial x} + 2 \frac{\partial \bar{w}}{\partial x}\right) \frac{\partial w}{\partial x}$$

$$\epsilon_y = \frac{\partial v}{\partial y} + \frac{w}{R} + \frac{1}{2} \left(\frac{\partial w}{\partial y} + 2 \frac{\partial \bar{w}}{\partial y}\right) \frac{\partial w}{\partial y}$$

$$\gamma_{xy} = \frac{\partial u}{\partial y} + \frac{\partial v}{\partial x} + \frac{\partial w}{\partial x} \cdot \frac{\partial w}{\partial y} + \frac{\partial w}{\partial y} \cdot \frac{\partial \bar{w}}{\partial x} + \frac{\partial w}{\partial x} \cdot \frac{\partial \bar{w}}{\partial y} \tag{14}$$

the stress resultants are given in terms of displacement as:

$$(1-\nu^2)\frac{N_x}{Et} = \left[\frac{\partial u}{\partial x} + \frac{1}{2}\left(\frac{\partial w}{\partial x} + 2\frac{\partial \overline{w}}{\partial x}\right)\frac{\partial w}{\partial x}\right] +$$

$$+\nu\left[\frac{\partial v}{\partial y} + \frac{w}{R} + \frac{1}{2}\left(\frac{\partial w}{\partial y} + 2\frac{\partial \overline{w}}{\partial y}\right)\frac{\partial w}{\partial y}\right]$$

$$(1-\nu^2)\frac{N_y}{Et} = \nu\left[\frac{\partial u}{\partial x} + \frac{1}{2}\left(\frac{\partial w}{\partial x} + 2\frac{\partial \overline{w}}{\partial x}\right)\frac{\partial w}{\partial x}\right] +$$

$$+\left[\frac{\partial v}{\partial y} + \frac{w}{R} + \frac{1}{2}\left(\frac{\partial w}{\partial y} + 2\frac{\partial \overline{w}}{\partial y}\right)\frac{\partial w}{\partial y}\right]$$

$$2(1+\nu)\frac{N_{xy}}{Et} = \frac{\partial u}{\partial y} + \frac{\partial v}{\partial x} + \left[\frac{\partial w}{\partial x} \cdot \frac{\partial (w+\overline{w})}{\partial y}\right] + \frac{\partial w}{\partial y} \cdot \frac{\partial \overline{w}}{\partial x} \qquad (15)$$

Since the displacements are now fully determined, one has that:

$$N_x = \frac{Et}{1-\nu^2}\left\{N_1 + N_5 \cos 2\ell\frac{y}{R} + N_6 \sin k\pi\frac{x}{L}\cos\ell\frac{y}{R}\right.$$

$$+N_8 \sin(i+k)\pi\frac{x}{L}\cos\ell\frac{y}{R} +$$

$$\left.+N_9 \sin(i-k)\pi\frac{x}{L}\cos\ell\frac{y}{R}\right\} \qquad (16)$$

$$N_y = \frac{Et}{1-\nu^2}\left\{M_1 + M_2 \cos i\pi\frac{x}{L} + M_3 \cos 2k\pi\frac{x}{L}\right.$$

$$+M_6 \sin k\pi\frac{x}{L}\cos\ell\frac{y}{R} +$$

$$+M_8 \sin(i+k)\pi\frac{x}{L}\cos\ell\frac{y}{R} +$$

$$\left.+M_9 \sin(i-k)\pi\frac{x}{L}\cos\ell\frac{y}{R}\right\} \qquad (17)$$

$$N_{xy} = \frac{Et}{2(1+\nu)} \left\{ P_1 \cos k\pi \frac{x}{L} \sin \ell \frac{y}{R} + \right.$$

$$+ P_3 \cos(i+k)\pi \frac{x}{L} \sin \ell \frac{y}{R} +$$

$$\left. + P_4 \cos(i-k)\pi \frac{x}{L} \sin \ell \frac{y}{R} \right\} \qquad (18)$$

The coefficients N_i, M_i, and P_i are given in Appendix III.

In order to determine u_1, one must enforce that

$$\int_0^{2\pi R} [N_x(L, y) - \sigma t] \, dy = 0 \qquad (19)$$

$$N_x(L, y) = \frac{Et}{1-\nu^2} N_1 + \frac{Et}{1-\nu^2} N_5 \cos 2\ell \frac{y}{R}$$

therefore

$$N_1 = (1-\nu^2) \frac{\sigma}{E} \qquad (20)$$

Since the coefficient N_1 in equation (16) contains the as yet undetermined coefficient u_1, one has that:

$$u_1 = -\frac{\nu t}{R} \xi_3 - \frac{t^2}{2} \left(\frac{i\pi}{L}\right)^2 \left(\frac{1}{2} \xi_1^2 + \xi_1 \bar{\xi}_1\right)$$

$$- \frac{t^2}{4} \left[\left(\frac{k\pi}{L}\right)^2 + \nu \left(\frac{\ell}{R}\right)^2\right] \left(\frac{1}{2} \xi_2^2 + \xi_2 \bar{\xi}_2\right)$$

$$+ (1-\nu^2) \frac{\sigma}{E} \qquad (21)$$

Note that this means that N_x is given by

$$N_x = \sigma t + \left\{ \frac{Et}{1-\nu^2} N_5 \cos 2\ell \frac{y}{R} + \right.$$

$$\frac{Et}{1-\nu^2} N_6 \sin k\pi \frac{x}{L} \cos \ell \frac{y}{R} +$$

$$+ \frac{Et}{1-\nu^2} N_8 \sin(i+k)\pi \frac{x}{L} \cos \ell \frac{y}{R} +$$

$$\left. + \frac{Et}{1-\nu^2} N_9 \sin (i-k)\pi \frac{x}{L} \cos \ell \frac{y}{R} \right\} \qquad (22)$$

5. Potential Energy

It can be shown that the total potential energy can be written as (Ref. 4):

$$U = U_1 + U_2 + U_3 \qquad (23)$$

where:

U_1 = strain energy due to the bending moments (M_x, M_y, M_{xy})

U_2 = strain energy due to the straining of the middle surface by the membrane forces (N_x, N_y, N_{xy})

U_3 = work done by the load.

These terms are given by the integrals:

$$U_1 = \frac{Et^3}{24(1-\nu^2)} \int_o^{2\pi R} \int_o^L \left\{ (\kappa_{xx}+\kappa_{yy})^2 - 2(1-\nu)(\kappa_{xx}\kappa_{yy} - \kappa_{xy}^2) \right\} dx dy$$

$$U_2 = \frac{1}{2Et} \int_o^{2\pi R} \int_o^L \left\{ (N_x+N_y)^2 - 2(1+\nu)(N_x N_y - N_{xy}^2) \right\} dx dy$$

$$U_3 = - \int_o^{2\pi R} N_x(L, y) \int_o^L \frac{\partial u}{\partial x} dx\, dy \qquad (24)$$

But it is also true that

$$\kappa_{xx} = w,_{xx}$$

$$\kappa_{yy} = w,_{yy} \qquad c = \sqrt{3(1-\nu^2)}$$

$$\kappa_{xy} = w,_{xy}$$

thus the integral U_1 is given by

$$U_1 = \frac{Et^3}{8c^2} \int_0^{2\pi R} \int_0^{L} \Big\{ (w,_{xx} + w,_{yy})^2 - 2(1-\nu)(w,_{xx} \cdot w,_{yy} - w,^2_{xy}) \Big\} \, dxdy \qquad (25)$$

also

$$U_3 = t\sigma \int_0^{2\pi R} \Big\{ u(L, y) - u(0, y) \Big\} \, dy$$

yielding:

$$U_3 = 2\pi R t \sigma \, u_1 L \qquad (26)$$

The integrals U_1 and U_2 are readily integrable. It should be noted that many of the trigonometric forms which result from the various products have no contribution to the total potential energy. The result is as follows:

The total potential energy is given by

$$U = \frac{Et^5 \pi RL}{8c^2}\left\{\left(\frac{i\pi}{L}\right)^4 \xi_1^2 + \frac{1}{2}\left[\left(\frac{k\pi}{L}\right)^2 + \left(\frac{\ell}{R}\right)^2\right]^2 \xi_2^2\right\}$$

$$+ 2\pi RLt\sigma\left\{(1-\nu^2)\frac{\sigma}{E} - \frac{\nu t}{R}\xi_3 - \frac{t^2}{2}\left(\frac{i\pi}{L}\right)^2\left(\frac{1}{2}\xi_1^2 + \xi_1\bar{\xi}_1\right)\right.$$

$$\left. - \frac{t^2}{4}\left[\left(\frac{k\pi}{L}\right)^2 + \nu\left(\frac{\ell}{R}\right)^2\right]\left(\frac{1}{2}\xi_2^2 + \xi_2\bar{\xi}_2\right)\right\}$$

$$+ \frac{\pi RLEt}{(1-\nu^2)^2}\left\{N_1^2 + \frac{1}{2}N_5^2 + \frac{1}{4}N_6^2 + \frac{1}{4}N_8^2 + \frac{1}{4}N_9^2\right.$$

$$\left. + M_1^2 + \frac{1}{2}M_2^2 + \frac{1}{2}M_3^2 + \frac{1}{4}M_6^2 + \frac{1}{4}M_8^2 + \frac{1}{4}M_9^2\right\}$$

$$+ \frac{\pi RLEt}{8(1+\nu)}\left\{P_1^2 + P_3^2 + P_4^2\right\}$$

$$-\frac{2\nu\pi RLEt}{(1-\nu^2)^2}\left\{N_1M_1 + \frac{1}{4}N_6M_6 + \frac{1}{4}N_8M_8 + \frac{1}{4}N_9M_9\right\}$$

$$+ \frac{\pi RLEt}{(1-\nu^2)^2} M_2M_3 + \frac{\pi RLEt}{(1-\nu^2)^2} \frac{\left[\left(\frac{k\pi}{L}\right)^2 + \left(\frac{\ell}{R}\right)^2\right]^2}{2\left(\frac{\ell}{R}\right)^4} N_6N_9 \qquad (27)$$

As an expression of minimization of total potential energy, it is enforced that:

$$\frac{\partial U}{\partial \xi_1} = \frac{\partial U}{\partial \xi_2} = \frac{\partial U}{\partial \xi_3} = 0 \qquad (28)$$

Taking these partial derivatives and performing algebraic simplification yields the following three equations:

$$\xi_3 = \frac{\nu\lambda}{c} - \frac{c}{2}\beta^2\left(\frac{1}{2}\xi_2^2 + \xi_2\bar{\xi}_2\right) \tag{29}$$

$$(\lambda_{c_i}-\lambda)\xi_1 + C_8[\xi_1(\xi_2+\bar{\xi}_2) + \bar{\xi}_1\xi_2](\xi_2+\bar{\xi}_2) +$$

$$-C_1\left(\frac{1}{2}\xi_2^2+\xi_2\bar{\xi}_2\right) - C_{20}\,\xi_2(\xi_2+\bar{\xi}_2) = \lambda\bar{\xi}_1 \tag{30}$$

$$(\lambda_{c_k}-\lambda)\xi_2 + (C_9+C_{10})\left(\frac{1}{2}\xi_2^2+\xi_2\bar{\xi}_2\right)(\xi_2+\bar{\xi}_2) +$$

$$+C_{11}[\xi_1(\xi_2+\bar{\xi}_2) + \bar{\xi}_1\xi_2](\xi_1+\bar{\xi}_1) +$$

$$-C_4\,\xi_1(\xi_2+\bar{\xi}_2) - C_3[2\xi_2(\xi_1+\bar{\xi}_1) + \xi_1\bar{\xi}_2] = \lambda\bar{\xi}_2 \tag{31}$$

The coefficients in these equations are given in Appendix IV. Comparison of these equations to those of Arbocz and Babcock (Ref. 2) will reveal that they are identical if one reverses the sense of the radial displacement. (Ref. 2 uses positive inward vice outward.)

III. NUMERICAL ANALYSIS

1. Imperfection Model

As given in equation 6, the shell imperfections were assumed to be fully described by two modal components, one generalized axisymmetric mode and one asymmetric mode, i.e.,

$$\overline{w} = \overline{\xi}_1 t \cos i\pi \frac{x}{L} + \overline{\xi}_2 t \sin k\pi \frac{x}{L} \cos \ell \frac{y}{R}$$

Following the method of modeling given in reference 7, the amplitudes $\overline{\xi}_1$ and $\overline{\xi}_2$ are considered to have wave number dependence. Decay constants are introduced which decrease the amplitude with increasing wave number:

$$\overline{\xi}_1 = \frac{\overline{X}_A}{i^q} \tag{32}$$

$$\overline{\xi}_2 = \frac{\overline{X}}{k^r \ell^s} \tag{33}$$

Numerical values for the five parameters ($\overline{X}_A$, $\overline{X}$, q, r, s) were obtained experimentally by Arbocz and Babcock (Ref. 6) by fitting data for 31 different shells. In order to conduct a parametric study which would include values representative of that experimental work and be reasonably conservative of computational time, the following numerical values were used in the computations:

$\overline{X}_A$ = 0.05, 0.10, 0.20

$\overline{X}$ = -0.50, -1.00, -2.00

q = 1.0, 2.0, 3.0

r = 0.5, 1.0, 1.5

s = 0.5, 1.0, 1.5

Hence, 243 different imperfection amplitude models were used in computation. Eight different wave number combinations were used. As will be described subsequently, wave numbers were chosen such that quadratic terms (as well as cubic) were included in the analysis, and all asymmetric modes fell along the Koiter circle.

2. Shell Geometry and Material Properties

Throughout the numerical analysis, the geometry and material properties of the shell were held constant. The following numerical values were used:

$R = 4.00$

$L = 7.00$

$t = 4.64 \times 10^{-3}$

$\nu = 0.30$

3. Wave Numbers and Mode Shape Parameters

The quadratic terms in the buckling equations will vanish identically unless the restriction $i = 2k$ is enforced. Without the quadratic terms, these equations describe a structure insensitive to imperfections. Accordingly, the relationship $i = 2k$ was maintained in all calculations.

The wave numbers of the asymmetric mode term were chosen so that this mode corresponded to one of the so-called classical modes of the Koiter circle. This insures minimization of the asymmetric buckling load. For a discussion of this topic, the reader is referred to Imbert (Ref. 7). The Koiter circle is defined by the relationship

$$a_k^2 - a_k + \beta^2 = 0$$

or $$\beta^2 = a_k(1-a_k) \tag{34}$$

with the restriction that for positive, nonzero ℓ

$$a_k < 1$$

In practice, the computational scheme was coded to perform the following operations:

(1) The wave number k was entered (a whole number) along with shell geometry and properties.

(2) The mode shape parameter a_k was computed.

(3) β was computed based upon this computed value of a_k using equation 34.

(4) The wave number ℓ was computed from the value of β, then rounded to the nearest integer value.

(5) β was then recomputed based upon the rounded value of ℓ. This value was then used to compute all coefficients of the buckling equations.

Accordingly, the values of a_k and β were such that they were very close to but not exactly on the Koiter circle.

4. Numerical Procedure

Equation 30 can be solved for ξ_1 as follows:

$$\xi_1 = \frac{(\psi_3+\lambda\psi_4)}{(\psi_6-\lambda)} \tag{35}$$

The expressions for the terms ψ_i are given below. Using this expression for the displacement amplitude ξ_1, the second buckling equation may be written as a cubic polynomial in λ:

$$\lambda^3 + E_1 \lambda^2 + E_2 \lambda + E_3 = 0 \tag{36}$$

The coefficients E_i are given by:

$$E_1 = (\psi_1 - 2\psi_6) + \psi_4(\psi_2\psi_4 - \psi_5)$$

$$E_2 = \psi_6(\psi_6 - 2\psi_1 + \psi_4\psi_5) + \psi_3(2\psi_2\psi_4 - \psi_5)$$

$$E_3 = \psi_6(\psi_1\psi_6 + \psi_3\psi_5) + \psi_2\psi_3^2$$

The expressions for ψ_i are as follows:

$$\psi_1 = -\frac{\lambda_{c_k}\xi_2}{(\xi_2+\bar{\xi}_2)} - (C_9+C_{10})(\tfrac{1}{2}\xi_2^2+\xi_2\bar{\xi}_2)$$

$$-\frac{C_{11}\bar{\xi}_1^2\xi_2}{(\xi_2+\bar{\xi}_2)} + \frac{2C_3\bar{\xi}_1\xi_2}{(\xi_2+\bar{\xi}_2)}$$

$$\psi_2 = -C_{11}$$

$$\psi_3 = C_1(\tfrac{1}{2}\xi_2^2+\xi_2\bar{\xi}_2) + C_{20}\xi_2(\xi_2+\bar{\xi}_2)$$

$$-C_8\bar{\xi}_1\xi_2(\xi_2+\bar{\xi}_2)$$

$$\psi_4 = \bar{\xi}_1$$

$$\psi_5 = - \frac{C_{11}\bar{\xi}_1(2\xi_2+\bar{\xi}_2)}{(\xi_2+\bar{\xi}_2)} + \frac{C_3(2\xi_2+\bar{\xi}_2)}{(\xi_2+\bar{\xi}_2)} + C_4$$

$$\psi_6 = \lambda_{c_i} + C_8(\xi_2+\bar{\xi}_2)^2$$

Since the imperfection amplitudes were given by equations 32 and 33, and the mode shape parameters determined as in paragraph 3 above, one then has a polynomial of the form:

$$\lambda^3 + E_1(\xi_2)\lambda^2 + E_2(\xi_2)\lambda + E_3(\xi_2) = 0$$

The computational scheme was coded to solve for the buckling load as follows:

(1) The displacement amplitude ξ_2 was incremented from the origin, using very small steps.

(2) The polynomial was solved to obtain the lowest real root.

(3) The slope of the λ vs ξ_2 trace was then computed.

(4) The value of λ at which one first attains a zero slope was specified as the buckling load.

IV. DISCUSSION OF NUMERICAL RESULTS AND RECOMMENDATIONS

1. The Effect of Varying the Axisymmetric Model Parameters ($\bar{X}_A$ and q)

As shown by figures 3 through 8, the traces of buckling load versus wave number for models which have q = 2.0 and 3.0 coalesce, regardless of the value of $\bar{X}_A$. The reader is referred to Table III for a comparison of the numerical values listed for models 49, 76, 130, 157, 211, and 238 – all of which have identical asymmetric model parameters. Loads for these models are plotted on figure 5. For these six models, the spread between the highest and lowest calculated buckling load is 0.01300 for k = 1.0, decreasing by a factor of roughly one half as wave number increases by two, to a spread of 0.00194 at k = 14.0. This behavior is repeated for other cases (a total of 27 plots were possible of the type shown in figures 3 through 8). In more understandable terms, it is recalled that the decay constant q operates on the wave number i, and that i = 2k. It is also true that the axisymmetric amplitudes are assumed to be smaller numerically than the asymmetric amplitudes, and that the decay rate q is higher (2.0 and 3.0) than assumed values for r and s (1.5 is the highest). For the cases where q is 2.0 or 3.0 therefore, the axisymmetric imperfections are not only small in comparison to the asymmetric models, but the computed loads show that changes in the parameters $\bar{X}_A$ and q produce only very small changes in the algebraic equations, i.e., in this case the coupling is weak.

Using numerical values for comparison, in figure 5, models 76 and 211 are plotted. Imperfection amplitudes for these cases are:

for $k = 1.0$

model 76	model 211
$\bar{\xi}_1 = \frac{0.05}{(2)^3} = 0.00625$	$\bar{\xi}_1 = \frac{0.20}{(2)^2} = 0.05$
$\bar{\xi}_2 = \frac{-2.00}{(10)^{0.5}} = -0.63246$	$\bar{\xi}_2 = -0.63246$
$\lambda = 0.74368$	$\lambda = 0.73068$

for $k = 14.0$

model 76	model 211
$\bar{\xi}_1 = \frac{0.05}{(28)^3} = 0.00000$	$\bar{\xi}_1 = \frac{0.20}{(28)^2} = 0.00026$
$\bar{\xi}_2 = \frac{-2.00}{(14)^{1.0}(27)^{0.5}} = -0.02749$	$\bar{\xi}_2 = -0.02749$
$\lambda = 0.80224$	$\lambda = 0.80030$

Of the six models shown on figure 5 with $q = 2.0$ and 3.0, model 76 has the smallest $\bar{\xi}_1$ and model 211 the largest.

For a given asymmetric model, changes in the axisymmetric model do not change the sensitivity of the shell to long versus short wave imperfections. It is seen on these plots that as the axisymmetric imperfection amplitudes increase, the traces shift downward, but do not appreciably change in curvature.

Because of the observed behavior of the data for q = 2.0 and 3.0, it was possible to neglect the data for 135 of the 243 models as being repetitive. Hence it is possible to show all significant data on twelve figures, each having nine common traces.

2. The Asymmetric Model — the Effect of Varying $\overline{X}$

As can be seen in figures 9 through 20, as $\overline{X}$ increases, a translation downward of the buckling load trace occurs, without appreciably altering the curvature of the trace. The behavior is very similar to the case for varying $\overline{X}_A$, although somewhat more pronounced.

In the range of values chosen for $\overline{X}$, changes in this parameter do reduce the buckling load, but do not influence the sensitivity of the shell to long versus short wave imperfections. It was also noticeable that as $\overline{X}$ becomes large, there is some tendency for short wave sensitive structures to shift the wave number for minimum buckling load from k = 14 (or greater) to k = 11. This can also be seen in Table III where underlined loads are in the column for k = 12. One should realize, of course, that while the lowest buckling loads listed in Table III or shown on the figures are at k = 14, it is certainly true that in some cases buckling may be dominated by a higher wave number. However, no data are presented for these cases.

3. The Asymmetric Model — the Effect of Varying s

As can be seen by comparing figures 21 through 32, as s is increased, all other parameters held constant, the traces tend to collapse and shift upward, with curvature changes occurring which

shift the minimum buckling load to short wave sensitivity. Only in the cases where the axisymmetric imperfections are small and decay rapidly ($\overline{X}_A = 0.05$; $q = 2.0, 3.0$) is low wave number (long wave) buckling observed when s gets large (1.5). In other cases, since s is the decay rate operating on the circumferential wave number ℓ, and since ℓ varies from 10 to 27, a high value of s tends to make the asymmetric imperfection amplitude nearly equal to the axisymmetric imperfection amplitude. In that case, buckling is dominated by classical short wave imperfections.

It would perhaps be clearer to review the meaning of the various decay rates and the numerical range of wave numbers on which these decay rates operate. For the asymmetric model, the decay rate r operates on the axial wave number, k, which ranges from 1.0 to 14.0. The decay rate s operates on the circumferential wave number, ℓ, which in this case varies from 10.0 to 27.0. Both r and s were varied from 0.5 to 1.5. If both decay rates have the value 0.5, then at k = 1, the asymmetric imperfection amplitude is given by:

$$\xi_2 = \frac{\overline{X}}{(1)^{0.5}(10)^{0.5}}$$

At k = 14, the same term is given by:

$$\xi_2 = \frac{\overline{X}}{(14)^{0.5}(27)^{0.5}}$$

That is, the axial decay rate r decreases the amplitude by a factor of approximately 4, while the circumferential decay rate s does the same by a factor of less than 2 in going from low wave numbers to

high wave numbers.

For r and s equal to 1.0, the asymmetric imperfection amplitude is decreased by a factor of 14 for r, while for s this factor is less than 3. At r and s equal to 1.5, the effect is even greater, as the decay with circumferential wave number is much greater than that for axial wave number.

4. The Asymmetric Model – the Effect of Varying r

Of all the parameters in the imperfection models, the parameter r was found to have the greatest influence in shifting the sensitivity of the shell from classical short wave imperfections to long wave imperfections. As can be seen in figures 9 through 20, if the decay of asymmetric imperfections with axial wave number is relatively low (r = 0.5), then buckling is always dominated by short wave imperfections, regardless of variations of the other four parameters. As r is increased to 1.5, many models show a shift to long wave sensitivity, the greatest sensitivity occurring when $\overline{X}$ and r are both large (2.0 and 1.5 respectively).

5. Items Which Induce Short Wave Imperfection Sensitivity

   a. If the decay of asymmetric imperfections with increasing axial wave number is relatively slow (r = 0.5), then buckling is dominated by short wave imperfections, regardless of other factors.

   b. If the axisymmetric imperfections are large and decay slowly in comparison to the asymmetric imperfections, then short wave imperfections dominate (compare figures 19 and 20 to figures 13 and 14).

c. If the asymmetric imperfections are nearly equal in magnitude to the axisymmetric imperfections, then buckling is dominated by short wave imperfections. The important parameter in causing the axisymmetric imperfection to have a significant value is the decay rate q.

6. Items Which Induce Long Wave Imperfection Sensitivity

a. If the decay of axisymmetric imperfections with increasing axial wave number of this mode is relatively high ($q = 2.0, 3.0$) and the decay of the asymmetric imperfections is high ($r = 1.0, 1.5$), then buckling is dominated by long wave imperfections. If however, the decay of asymmetric imperfections with increasing circumferential wave number gets sufficiently large ($s = 1.5$, $\overline{X} = 0.5$) then this effect is lost. This is, however, not an interesting case, for in realistic terms, this means that the imperfections are virtually non-existent — the decay rates are simply too high.

b. With large axisymmetric imperfections decaying slowly with wave number, it is necessary to have large asymmetric imperfections decaying rapidly with axial wave number and slowly with circumferential wave number to have long wave dominance. The most striking case of long wave dominance occurred when $\overline{X}$ and r were both large.

7. Summary

Experimental evidence shows that imperfection amplitudes tend to decrease with wave number. The rate of decrease varies from shell to shell and covers a fairly wide range. If the decay constant of the axisymmetric imperfection is greater than one, then the buckling load becomes insensitive to variations of the decay constant in this imperfection.

The decay of the asymmetric imperfection amplitude with wave number is governed by two parameters. The axial wave parameter appears to be the more important parameter in governing the critical buckling modes. If this parameter is between zero and somewhat greater than one half, the shell behavior is dominated by short waves. This results since the size of the imperfection going from $k = 1.0$ to $k = 14.0$ is decreased by only a factor of approximately 4. Due to the greater imperfection sensitivity of modes with α_k and β close to 0.5, this behavior is to be expected. On the other end of the scale, if r is one to one and one half, the longer wave imperfections tend to be more important. This is not true if the decay with circumferential wave number gets sufficiently large. The behavior between these two extremes is less one sided, being sensitive to the influence of the decay of the imperfection with circumferential wave number, the size of the axisymmetric imperfection, and the axisymmetric imperfection decay rate. The lack of a clear cut dominance of short or long wave imperfections in this range of r is unfortunate since much of the available experimental data fall in this range. From an experimental point of view, the

range of r is not too great. However, in this range of r the behavior is sensitive to all of the other parameters in the model and the effects must be sorted out with care.

8. Recommendations

The numerical data generated for this study indicates that further investigation of the decay rate parameters would be enlightening. It is clear that one could interpolate between the curves obtained to gain information regarding behavior of shells with different values of the parameters $\overline{X}_A$ and $\overline{X}$ within the range of values used herein, and that the parameter q is relatively uninteresting (if greater than one). However, more attention could be devoted to the decay rates r and s, particularly in view of the fact that experimentally derived values for these parameters are scattered widely between the values 1.0 and 1.5. It is apparent that the nature of shell sensitivity to imperfections changes fairly rapidly within this range of those parameters.

REFERENCES

1. Fung, Y. C. and Sechler, E. E.: Instability of Thin Elastic Shells, Structural Mechanics, Pergamon Press, 1960.

2. Arbocz, J. and Babcock, C. D.: The Effect of General Imperfections on the Buckling of Cylindrical Shells, J. of Appl. Mech., March 1969.

3. Hutchinson, T.: Axial Buckling of Pressurized Imperfect Cylindrical Shells, AIAA J., Vol. 3, Aug. 1965.

4. Kármán, T. von and Tsien, H. S.: The Buckling of Thin Cylindrical Shells under Axial Compression, J. Aeronautical Sci., Vol. 8, No. 8, p. 302, 1941.

5. Donnell, L. H.: A New Theory for the Buckling of Thin Cylinders under Axial Compression and Bending. Trans. of A. S. M. E., Vol. 56, p. 795, Nov. 1934.

6. Arbocz, J. and Babcock, C. D.: On the Role of Imperfections in Shell Buckling, Paper presented at the XIII IUTAM Congress of Theoretical and Applied Mechanics, Moscow, Aug. 1972.

7. Imbert, J.: The Effect of Imperfections on the Buckling of Cylindrical Shells. Aeronautical Engineer Thesis, California Institute of Technology, June 1971.

APPENDIX I

Operator Coefficients

$$A_1 = t^2\left(\frac{i\pi}{L}\right)^3 \left(\frac{1}{2}\xi_1^2 + \xi_1\bar{\xi}_1\right)$$

$$A_2 = -\frac{\nu t}{R}\left(\frac{i\pi}{L}\right)\xi_1$$

$$A_3 = -\frac{t^2}{2}\left(\frac{k\pi}{L}\right)\left[\left(\frac{k\pi}{L}\right)^2 - \nu\left(\frac{\ell}{R}\right)^2\right]\left(\frac{1}{2}\xi_2^2+\xi_2\bar{\xi}_2\right)$$

$$A_4 = \frac{\nu t}{R}\left(\frac{k\pi}{L}\right)\xi_2$$

$$A_5 = -\frac{t^2}{2}\left(\frac{k\pi}{L}\right)\left[\left(\frac{k\pi}{L}\right)^2 + \left(\frac{\ell}{R}\right)^2\right]\left(\frac{1}{2}\xi_2^2 + \xi_2\bar{\xi}_2\right)$$

$$A_6 = -\frac{t^2}{2}\left(\frac{i\pi}{L}\right)\left[\left(\frac{k\pi}{L}\right)(i+k)\frac{\pi}{L} + \frac{(1-\nu)}{2}\left(\frac{\ell}{R}\right)^2\right]\cdot\left[\xi_1(\xi_2+\bar{\xi}_2)+\bar{\xi}_1\xi_2\right]$$

$$A_7 = -\frac{t^2}{2}\left(\frac{i\pi}{L}\right)\left[\left(\frac{k\pi}{L}\right)(i-k)\frac{\pi}{L} - \frac{(1-\nu)}{2}\left(\frac{\ell}{R}\right)^2\right]\cdot\left[\xi_1(\xi_2+\bar{\xi}_2)+\bar{\xi}_1\xi_2\right]$$

$$B_1 = -\frac{t^2}{2}\left(\frac{\ell}{R}\right)\left[\nu\left(\frac{k\pi}{L}\right)^2 - \left(\frac{\ell}{R}\right)^2\right]\left(\frac{1}{2}\xi_2^2 + \xi_2\bar{\xi}_2\right)$$

$$B_2 = -\frac{t^2}{2}\left(\frac{\ell}{R}\right)\left[\left(\frac{k\pi}{L}\right)^2 + \left(\frac{\ell}{R}\right)^2\right]\left(\frac{1}{2}\xi_2^2 + \xi_2\bar{\xi}_2\right)$$

$$B_3 = \frac{t^2}{4}\left(\frac{i\pi}{L}\right)\left(\frac{\ell}{R}\right)\left[(i+k)\frac{\pi}{L} - \nu(i-k)\frac{\pi}{L}\right]\cdot\left[\xi_1(\xi_2+\bar{\xi}_2)+\bar{\xi}_1\xi_2\right]$$

$$B_4 = \frac{t^2}{4}\left(\frac{i\pi}{L}\right)\left(\frac{\ell}{R}\right)\left[\nu(i+k)\frac{\pi}{L} - (i-k)\frac{\pi}{L}\right]\cdot\left[\xi_1(\xi_2+\bar{\xi}_2)+\bar{\xi}_1\xi_2\right]$$

$$B_5 = -\frac{t}{R}\left(\frac{\ell}{R}\right)\xi_2$$

APPENDIX II

Displacement Coefficients

$$a_1 = \frac{t^2}{4}\left(\frac{i\pi}{L}\right)\left(\frac{1}{2}\,\xi_1^2 + \xi_1\bar{\xi}_1\right)$$

$$a_2 = -\frac{\nu t}{R\left(\frac{i\pi}{L}\right)}\,\xi_1$$

$$a_3 = -\frac{t^2}{8}\,\frac{\left[\left(\frac{k\pi}{L}\right)^2 - \nu\left(\frac{\ell}{R}\right)^2\right]}{\left(\frac{k\pi}{L}\right)}\,\left(\frac{1}{2}\xi_2^2 + \xi_2\bar{\xi}_2\right)$$

$$a_4 = \frac{t}{R}\left(\frac{k\pi}{L}\right)\frac{\left[\nu\left(\frac{k\pi}{L}\right)^2 - \left(\frac{\ell}{R}\right)^2\right]}{\left[\left(\frac{k\pi}{L}\right)^2 + \left(\frac{\ell}{R}\right)^2\right]^2}\,\xi_2$$

$$a_5 = -\frac{t^2}{8}\left(\frac{k\pi}{L}\right)\left(\frac{1}{2}\xi_2^2 + \xi_2\bar{\xi}_2\right)$$

$$a_6 = \frac{\frac{t^2}{2}\left(\frac{i\pi}{L}\right)}{\left\{\left[(i+k)\frac{\pi}{L}\right]^2 + \left(\frac{\ell}{R}\right)^2\frac{(1-\nu)}{2}\right\}} \cdot \left\{\left(\frac{i\pi}{L}\right)\left(\frac{\ell}{R}\right)\left[(i+k)\frac{\pi}{L}\left(\frac{\ell}{R}\right)\frac{(1+\nu)}{2}\right] \cdot \right.$$

$$\cdot \frac{\left[\left[(i+k)\frac{\pi}{L}\right]^2 - \nu\left(\frac{\ell}{R}\right)^2\right]}{\left[\left[(i+k)\frac{\pi}{L}\right]^2 + \left(\frac{\ell}{R}\right)^2\right]^2}$$

$$\left. -\left[(i+k)\frac{\pi}{L}\right) + \frac{(1-\nu)}{2}\left(\frac{\ell}{R}\right)^2\right]\right\} \cdot \left[\xi_1(\xi_2+\bar{\xi}_2)+\bar{\xi}_1\xi_2\right]$$

$$a_7 = -\frac{t^2}{2}\left\{\frac{\left(\frac{i\pi}{L}\right)\left(\frac{k\pi}{L}\right)}{\left[(i-k)\frac{\pi}{L}\right]} + \frac{\left(\frac{i\pi}{L}\right)^2\left(\frac{\ell}{R}\right)^2}{\left[(i-k)\frac{\pi}{L}\right]} \cdot \frac{\left[\nu\left[(i-k)\frac{\pi}{L}\right]^2 - \left(\frac{\ell}{R}\right)^2\right]}{\left[\left[(i-k)\frac{\pi}{L}\right]^2 + \left(\frac{\ell}{R}\right)^2\right]^2}\right\} \cdot$$

$$\cdot \left[\xi_1(\xi_2+\bar{\xi}_2) + \bar{\xi}_1\xi_2\right]$$

$$b_1 = -\frac{t^2}{8}\ \frac{[\nu(\frac{k\pi}{L})^2-(\frac{\ell}{R})^2]}{(\frac{\ell}{R})}\ (\frac{1}{2}\ \xi_2^2 + \xi_2\bar{\xi}_2)$$

$$b_5 = -\frac{t}{R}(\frac{\ell}{R})\ \frac{[(\frac{\ell}{R})^2+(\frac{k\pi}{L})^2(\nu+2)]}{[(\frac{k\pi}{L})^2+(\frac{\ell}{R})^2]^2}\ \xi_2$$

$$b_2 = -\frac{t^2}{8}(\frac{\ell}{R})(\frac{1}{2}\xi_2^2 + \xi_2\bar{\xi}_2)$$

$$b_3 = \frac{t^2}{2}\ \frac{(\frac{i\pi}{L})^2(\frac{\ell}{R})\left[[(i+k)\frac{\pi}{L}]^2-\nu(\frac{\ell}{R})^2\right]}{\left[[(i+k)\frac{\pi}{L}]^2+(\frac{\ell}{R})^2\right]^2}\ \cdot\ [\xi_1(\xi_2+\bar{\xi}_2)+\bar{\xi}_1\xi_2]$$

$$b_4 = \frac{t^2}{2}(\frac{i\pi}{L})^2(\frac{\ell}{R})\ \frac{\left[[(i-k)\frac{\pi}{L}]^2-\nu(\frac{\ell}{R})^2\right]}{\left[[(i-k)\frac{\pi}{L}]^2+(\frac{\ell}{R})^2\right]^2}\ \cdot\ [\xi_1(\xi_2+\bar{\xi}_2)+\bar{\xi}_1\xi_2]$$

APPENDIX III

Stress Resultant Coefficients

$$N_1 = u_1 + \frac{\nu t}{R}\,\xi_3 + \frac{t^2}{2}\left(\frac{i\pi}{L}\right)^2\left(\frac{1}{2}\,\xi_1^2 + \xi_1\bar{\xi}_1\right)$$

$$+ \frac{t^2}{4}\left[\left(\frac{k\pi}{L}\right)^2 + \nu\left(\frac{\ell}{R}\right)^2\right]\left(\frac{1}{2}\,\xi_2^2 + \xi_2\bar{\xi}_2\right)$$

$$N_1 = (1-\nu^2)\,\frac{\sigma}{E} \qquad \text{(when } u_1 \text{ is substituted)}$$

$$N_5 = \frac{t^2}{4}\,(1-\nu^2)\left(\frac{k\pi}{L}\right)^2\left(\frac{1}{2}\,\xi_2^2 + \xi_2\bar{\xi}_2\right)$$

$$N_6 = \frac{t}{R}\,\frac{(1-\nu^2)\left(\frac{k\pi}{L}\right)^2\left(\frac{\ell}{R}\right)^2}{\left[\left(\frac{k\pi}{L}\right)^2 + \left(\frac{\ell}{R}\right)^2\right]^2}\,\xi_2$$

$$N_8 = \frac{t^2}{2}\,\frac{\left(\frac{i\pi}{L}\right)^2\left(\frac{\ell}{R}\right)^4(1-\nu^2)}{\left[\left[(i+k)\frac{\pi}{L}\right]^2 + \left(\frac{\ell}{R}\right)^2\right]^2}\left[\xi_1(\xi_2+\bar{\xi}_2) + \bar{\xi}_1\xi_2\right]$$

$$N_9 = -\frac{t^2}{2}\,\frac{\left(\frac{i\pi}{L}\right)^2\left(\frac{\ell}{R}\right)^4(1-\nu^2)}{\left[\left[(i-k)\frac{\pi}{L}\right]^2 + \left(\frac{\ell}{R}\right)^2\right]^2}\left[\xi_1(\xi_2+\bar{\xi}_2) + \bar{\xi}_1\xi_2\right]$$

$$M_1 = (1-\nu^2)\frac{t}{R}\,\xi_3 + \nu(1-\nu^2)\,\frac{\sigma}{E} + \frac{t^2}{4}\left(\frac{\ell}{R}\right)^2(1-\nu^2)\left(\frac{1}{2}\,\xi_2^2 + \xi_2\bar{\xi}_2\right)$$

$$M_2 = (1-\nu^2)\frac{t}{R}\,\xi_1$$

$$M_3 = -(1-\nu^2)\,\frac{t^2}{4}\left(\frac{\ell}{R}\right)^2\left(\frac{1}{2}\,\xi_2^2 + \xi_2\bar{\xi}_2\right)$$

$$M_6 = \frac{(1-\nu^2)\frac{t}{R}\left(\frac{k\pi}{L}\right)^4}{\left[\left(\frac{k\pi}{L}\right)^2+\left(\frac{\ell}{R}\right)^2\right]^2}\ \xi_2$$

$$M_8 = \frac{t^2}{2}\ \frac{(1-\nu^2)\left(\frac{i\pi}{L}\right)^2\left[(i+k)\frac{\pi}{L}\right]^2\left(\frac{\ell}{R}\right)^2}{\left[\left[(i+k)\frac{\pi}{L}\right]^2+\left(\frac{\ell}{R}\right)^2\right]^2}\ \left[\xi_1(\xi_2+\bar{\xi}_2)+\bar{\xi}_1\xi_2\right]$$

$$M_9 = -\frac{t^2}{2}\ \frac{(1-\nu^2)\left(\frac{i\pi}{L}\right)^2\left[(i-k)\frac{\pi}{L}\right]^2\left(\frac{\ell}{R}\right)^2}{\left[\left[(i-k)\frac{\pi}{L}\right]^2+\left(\frac{\ell}{R}\right)^2\right]^2}\ \left[\xi_1(\xi_2+\bar{\xi}_2)+\bar{\xi}_1\xi_2\right]$$

$$P_1 = -\frac{t}{R}\ \frac{\left(\frac{k\pi}{L}\right)^3\left(\frac{\ell}{R}\right)\ \ 2(1+\nu)}{\left[\left(\frac{k\pi}{L}\right)^2+\left(\frac{\ell}{R}\right)^2\right]^2}\ \xi_2$$

$$P_3 = -(1+\nu)\ \frac{t^2\left(\frac{i\pi}{L}\right)^2(i+k)\ \frac{\pi}{L}\left(\frac{\ell}{R}\right)^3}{\left[\left[(i+k)\ \frac{\pi}{L}\right]^2+\left(\frac{\ell}{R}\right)^2\right]^2}\ \left[\xi_1(\xi_2+\bar{\xi}_2)+\bar{\xi}_1\xi_2\right]$$

$$P_4 = t^2\ \frac{(1+\nu)\left(\frac{i\pi}{L}\right)^2\left(\frac{\ell}{R}\right)^3\left[(i-k)\ \frac{\pi}{L}\right]}{\left[\left[(i-k)\ \frac{\pi}{L}\right]^2+\left(\frac{\ell}{R}\right)^2\right]^2}\ \left[\xi_1(\xi_2+\bar{\xi}_2)+\bar{\xi}_1\xi_2\right]$$

APPENDIX IV

Mode Shape Parameter Coefficients

$$\lambda_{c_i} = \frac{1}{2}\left(\alpha_i^2 + \frac{1}{\alpha_i^2}\right)$$

$$\lambda_{c_k} = \frac{1}{2}\left[\frac{(\alpha_k^2+\beta^2)^2}{\alpha_k^2} + \frac{\alpha_k^2}{(\alpha_k^2+\beta^2)^2}\right]$$

$$C_1 = \frac{c\beta^2}{4\alpha_i^2}, \quad \text{for } i = 2k \quad (\text{if } i \neq 2k,\ C_1 = 0)$$

$$C_3 = \frac{c\alpha_i^2\beta^2}{2[\overline{\gamma}_k]}, \quad \text{for } i = 2k \quad (\text{if } i \neq 2k,\ C_3 = 0)$$

$$C_4 = \frac{c\beta^2}{2\alpha_k^2}, \quad \text{for } i = 2k \quad (\text{if } i \neq 2k,\ C_4 = 0)$$

$$C_8 = \frac{c^2}{4}\ \alpha_i^2\beta^4\ \left\{\frac{1}{\overline{\gamma}_{i+k}} + \frac{1}{\overline{\gamma}_{i-k}}\right\}$$

$$C_9 = \frac{c^2\beta^4}{4\alpha_k^2}$$

$$C_{10} = \frac{c^2}{4}\alpha_k^2$$

$$C_{11} = \frac{c^2}{2}\ \frac{\alpha_i^4\beta^4}{\alpha_k^2}\ \left\{\frac{1}{\overline{\gamma}_{i+k}} + \frac{1}{\overline{\gamma}_{i-k}}\right\}$$

$$C_{20} = \frac{c}{4}\ \frac{\alpha_k^2\beta^2}{\overline{\gamma}_k}, \quad \text{for } i = 2k \quad (\text{if } i \neq 2k,\ C_{20} = 0)$$

$$\alpha_i^2 = i^2\,\frac{Rt}{2c}\left(\frac{\pi}{L}\right)^2$$

$$\alpha_k^2 = k^2\,\frac{Rt}{2c}\left(\frac{\pi}{L}\right)^2$$

$$\alpha_{i+k}^2 = \frac{Rt}{2c}\left[(i+k)\frac{\pi}{L}\right]^2$$

$$\alpha_{i-k}^2 = \frac{Rt}{2c}\left[i-k)\,\frac{\pi}{L}\right]^2$$

$$\beta^2 = \frac{Rt}{2c}\left(\frac{\ell}{R}\right)^2$$

$$\overline{\gamma}_k = (\alpha_k^2 + \beta^2)^2$$

$$\overline{\gamma}_{i+k} = (\alpha_{i+k}^2 + \beta^2)^2$$

$$\overline{\gamma}_{i-k} = (\alpha_{i-k}^2 + \beta^2)^2$$

TABLE I

Summary of Mode Selection

k	i	l	a_k	β
1	2	10	0.03363	0.18736
2	4	13	0.06727	0.24357
4	8	18	0.13454	0.33725
6	12	21	0.20181	0.39345
8	16	24	0.26908	0.44966
10	20	25	0.33635	0.46840
12	24	26	0.40361	0.48713
14	28	27	0.47088	0.50587

TABLE II

Imperfection Model Summary

Model Number	$\overline{X}_A$	q	$\overline{X}$	r	s
1	0.05	1.0	0.5	0.5	0.5
2	0.05	1.0	0.5	0.5	1.0
3	0.05	1.0	0.5	0.5	1.5
4	0.05	1.0	0.5	1.0	0.5
5	0.05	1.0	0.5	1.0	1.0
6	0.05	1.0	0.5	1.0	1.5
7	0.05	1.0	0.5	1.5	0.5
8	0.05	1.0	0.5	1.5	1.0
9	0.05	1.0	0.5	1.5	1.5
10	0.05	1.0	1.0	0.5	0.5
11	0.05	1.0	1.0	0.5	1.0
12	0.05	1.0	1.0	0.5	1.5
13	0.05	1.0	1.0	1.0	0.5
14	0.05	1.0	1.0	1.0	1.0
15	0.05	1.0	1.0	1.0	1.5
16	0.05	1.0	1.0	1.5	0.5
17	0.05	1.0	1.0	1.5	1.0
18	0.05	1.0	1.0	1.5	1.5
19	0.05	1.0	2.0	0.5	0.5
20	0.05	1.0	2.0	0.5	1.0
21	0.05	1.0	2.0	0.5	1.5
22	0.05	1.0	2.0	1.0	0.5

TABLE II (Cont'd)

Imperfection Model Summary

Model Number	$\overline{X}_A$	q	$\overline{X}$	r	s
23	0.05	1.0	2.0	1.0	1.0
24	0.05	1.0	2.0	1.0	1.5
25	0.05	1.0	2.0	1.5	0.5
26	0.05	1.0	2.0	1.5	1.0
27	0.05	1.0	2.0	1.5	1.5
28	0.05	2.0	0.5	0.5	0.5
29	0.05	2.0	0.5	0.5	1.0
30	0.05	2.0	0.5	0.5	1.5
31	0.05	2.0	0.5	1.0	0.5
32	0.05	2.0	0.5	1.0	1.0
33	0.05	2.0	0.5	1.0	1.5
34	0.05	2.0	0.5	1.5	0.5
35	0.05	2.0	0.5	1.5	1.0
36	0.05	2.0	0.5	1.5	1.5
37	0.05	2.0	1.0	0.5	0.5
38	0.05	2.0	1.0	0.5	1.0
39	0.05	2.0	1.0	0.5	1.5
40	0.05	2.0	1.0	1.0	0.5
41	0.05	2.0	1.0	1.0	1.0
42	0.05	2.0	1.0	1.0	1.5
43	0.05	2.0	1.0	1.5	0.5
44	0.05	2.0	1.0	1.5	1.0

TABLE II (Cont'd)

Imperfection Model Summary

Model Number	$\overline{X}_A$	q	$\overline{X}$	r	s
45	0.05	2.0	1.0	1.5	1.5
46	0.05	2.0	2.0	0.5	0.5
47	0.05	2.0	2.0	0.5	1.0
48	0.05	2.0	2.0	0.5	1.5
49	0.05	2.0	2.0	1.0	0.5
50	0.05	2.0	2.0	1.0	1.0
51	0.05	2.0	2.0	1.0	1.5
52	0.05	2.0	2.0	1.5	0.5
53	0.05	2.0	2.0	1.5	1.0
54	0.05	2.0	2.0	1.5	1.5
55	0.05	3.0	0.5	0.5	0.5
56	0.05	3.0	0.5	0.5	1.0
57	0.05	3.0	0.5	0.5	1.5
58	0.05	3.0	0.5	1.0	0.5
59	0.05	3.0	0.5	1.0	1.0
60	0.05	3.0	0.5	1.0	1.5
61	0.05	3.0	0.5	1.5	0.5
62	0.05	3.0	0.5	1.5	1.0
63	0.05	3.0	0.5	1.5	1.5
64	0.05	3.0	1.0	0.5	0.5
65	0.05	3.0	1.0	0.5	1.0
66	0.05	3.0	1.0	0.5	1.5
67	0.05	3.0	1.0	1.0	0.5

TABLE II (Cont'd)

Imperfection Model Summary

Model Number	$\overline{X}_A$	q	$\overline{X}$	r	s
68	0.05	3.0	1.0	1.0	1.0
69	0.05	3.0	1.0	1.0	1.5
70	0.05	3.0	1.0	1.5	0.5
71	0.05	3.0	1.0	1.5	1.0
72	0.05	3.0	1.0	1.5	1.5
73	0.05	3.0	2.0	0.5	0.5
74	0.05	3.0	2.0	0.5	1.0
75	0.05	3.0	2.0	0.5	1.5
76	0.05	3.0	2.0	1.0	0.5
77	0.05	3.0	2.0	1.0	1.0
78	0.05	3.0	2.0	1.0	1.5
79	0.05	3.0	2.0	1.5	0.5
80	0.05	3.0	2.0	1.5	1.0
81	0.05	3.0	2.0	1.5	1.5

Notes:

1. For models 82 through 162 inclusive, $\overline{X}_A$ becomes 0.10, all other parameters sequence as in models 1 through 81.

2. For models 163 through 243 inclusive, $\overline{X}_A$ becomes 0.20, all other parameters sequence as in models 1 through 81.

3. In all cases, the sign of the axisymmetric imperfection is positive (outward) while the asymmetric imperfection is always negative (inward).

TABLE III

Buckling Loads, λ_{crit}

Imperfection Model Number	Wave Number, k							
	1	2	4	6	8	10	12	14
1	0.88982	0.87412	0.85521	0.84301	0.82596	0.80884	0.79523	0.79485
2	0.94794	0.94232	0.93681	0.93395	0.92557	0.91224	0.89521	0.88588
3	0.97567	0.97224	0.96931	0.96899	0.96347	0.95294	0.93481	0.91984
4	0.88982	0.89824	0.90340	0.90630	0.90095	0.89147	0.87873	0.87377
5	0.94794	0.95299	0.95617	0.95855	0.95440	0.94513	0.92866	0.91562
6	0.97567	0.97686	0.97684	0.97812	0.97386	0.96489	0.94685	0.92979
7	0.88982	0.91767	0.93473	0.94288	0.94151	0.93473	0.92081	0.91044
8	0.94794	0.96152	0.96850	0.97232	0.96926	0.96116	0.94408	0.92804
9	0.97567	0.98052	0.98160	0.98318	0.97912	0.97055	0.95220	0.93386
10	0.82883	0.80768	0.78256	0.76625	0.74692	0.73071	0.72187	0.72796
11	0.91809	0.91229	0.90664	0.90267	0.89305	0.87850	0.86287	0.85726
12	0.96149	0.95917	0.95745	0.95716	0.95145	0.94016	0.92256	0.90979
13	0.82883	0.84430	0.85521	0.86039	0.85597	0.84784	0.83874	0.83920
14	0.91809	0.92896	0.93681	0.94081	0.93733	0.92813	0.91310	0.90315
15	0.96149	0.96644	0.96931	0.97155	0.96775	0.95877	0.94133	0.92566
16	0.82883	0.87412	0.90340	0.91646	0.91742	0.91224	0.90114	0.89494
17	0.91809	0.94232	0.95617	0.96240	0.96050	0.95294	0.93698	0.92292
18	0.96149	0.97224	0.97684	0.97955	0.97603	0.96766	0.94976	0.93217

TABLE III (Cont'd)

Buckling Loads, λ_{crit}

Imperfection Model Number	Wave Number, k							
	1	2	4	6	8	10	12	14
19	0.73804	0.70934	0.67699	0.65723	0.63824	0.62635	0.62545	0.64052
20	0.87192	0.86583	0.86014	0.85489	0.84421	0.82897	0.81591	0.81508
21	0.93925	0.93863	0.93881	0.93865	0.93275	0.92052	0.90384	0.89394
22	0.73804	0.76307	0.78256	0.79174	0.78987	0.78511	0.78179	0.78927
23	0.87192	0.89154	0.90664	0.91325	0.91100	0.90228	0.88950	0.88362
24	0.93925	0.95003	0.95745	0.96118	0.95813	0.94919	0.93270	0.91903
25	0.73804	0.80768	0.85521	0.87584	0.88071	0.87850	0.87162	0.87101
26	0.87192	0.91229	0.93681	0.94683	0.94680	0.94016	0.92594	0.91468
27	0.93925	0.95917	0.96931	0.97379	0.97115	0.96312	0.94589	0.92948
28	0.89454	0.88101	0.86324	0.85193	0.83626	0.82067	0.80825	0.80779
29	0.95302	0.94982	0.94583	0.94444	0.93878	0.92987	0.91873	0.91217
30	0.98093	0.98003	0.97874	0.98012	0.97804	0.97398	0.96742	0.95977
31	0.89454	0.90535	0.91201	0.91629	0.91337	0.90763	0.89972	0.89712
32	0.95302	0.96061	0.96543	0.96948	0.96863	0.96544	0.95945	0.95316
33	0.98093	0.98469	0.98636	0.98943	0.98882	0.98714	0.98364	0.97692
34	0.89454	0.92497	0.94373	0.95353	0.95528	0.95411	0.94955	0.94537
35	0.95302	0.96921	0.97792	0.98351	0.98403	0.98302	0.97980	0.97375
36	0.98093	0.98839	0.99118	0.99459	0.99428	0.99340	0.99128	0.98475

TABLE III (Cont'd)

Buckling Loads, λ_{crit}

Imperfection Model Number	Wave Number, k							
	1	2	4	6	8	10	12	14
37	0.83313	0.81397	0.78972	0.77397	0.75534	0.73972	0.73110	0.73679
38	0.92298	0.91952	0.91528	0.91260	0.90522	0.89386	0.88183	0.87746
39	0.96666	0.96684	0.96672	0.96807	0.96557	0.96002	0.95173	0.94441
40	0.83313	0.85092	0.86324	0.86960	0.86707	0.86150	0.85517	0.85672
41	0.92298	0.93635	0.94583	0.95142	0.95095	0.94698	0.94007	0.93501
42	0.96666	0.97418	0.97874	0.98273	0.98247	0.98038	0.97610	0.96943
43	0.83313	0.88101	0.91201	0.92663	0.93038	0.92987	0.92571	0.92391
44	0.92298	0.94982	0.96543	0.97341	0.97495	0.97398	0.97027	0.96471
45	0.96666	0.98003	0.98636	0.99088	0.99107	0.99019	0.98778	0.98144
46	0.74179	0.71475	0.68295	0.66339	0.64454	0.63265	0.63155	0.64619
47	0.87653	0.87263	0.86821	0.86401	0.85498	0.84170	0.83040	0.82983
48	0.94428	0.94609	0.94786	0.94922	0.94622	0.93877	0.92892	0.92256
49	0.74179	0.76896	0.78972	0.79985	0.79926	0.79598	0.79398	0.80177
50	0.87653	0.89859	0.91528	0.92337	0.92375	0.91918	0.91209	0.90927
51	0.94428	0.95762	0.96672	0.97217	0.97250	0.96990	0.96466	0.95849
52	0.74179	0.81397	0.86324	0.88531	0.89251	0.89386	0.89165	0.89377
53	0.87653	0.91952	0.94583	0.95756	0.96075	0.96002	0.95599	0.95171
54	0.94428	0.96684	0.97874	0.98501	0.98601	0.98518	0.98236	0.97630

TABLE III (Cont' d)

Buckling Loads, λ_{crit}

Imperfection Model Number	Wave Number, k							
	1	2	4	6	8	10	12	14
55	0.89691	0.88273	0.86425	0.85268	0.83691	0.82128	0.80882	0.80828
56	0.95558	0.95171	0.94697	0.94532	0.93963	0.93080	0.91985	0.91335
57	0.98358	0.98199	0.97993	0.98106	0.97898	0.97511	0.96916	0.96232
58	0.89691	0.90714	0.91310	0.91713	0.91416	0.90848	9.90070	0.89812
59	0.95558	0.96252	0.96660	0.97041	0.96954	0.96652	0.96105	0.95533
60	0.98358	0.98667	0.98756	0.99039	0.98979	0.98835	0.98574	0.98115
61	0.89691	0.92680	0.94486	0.95443	0.95617	0.95515	0.95101	0.94729
62	0.95558	0.97115	0.97911	0.98446	0.98498	0.98420	0.98180	0.97744
63	0.98358	0.99037	0.99239	0.99555	0.99525	0.99465	0.99363	0.99079
64	0.83531	0.81556	0.79063	0.77462	0.75587	0.74018	0.73150	0.73712
65	0.92545	0.92134	0.91637	0.91343	0.90600	0.89466	0.88269	0.87828
66	0.96926	0.96877	0.96789	0.96899	0.96648	0.96108	0.95321	0.94630
67	0.83531	0.85259	0.86425	0.87038	0.86778	0.86221	0.85590	0.85742
68	0.92545	0.93822	0.94697	0.95232	0.95183	0.94798	0.94140	0.93661
69	0.96296	0.97613	0.97993	0.98367	0.98342	0.98155	0.97802	0.97280
70	0.83531	0.88273	0.91310	0.92749	0.93120	0.93080	0.92689	0.92528
71	0.92545	0.95171	0.96660	0.97434	0.97588	0.97511	0.97207	0.96771
72	0.96926	0.98199	0.98756	0.99184	0.99203	0.99141	0.99001	0.98655

TABLE III (Cont'd)

Buckling Loads, λ_{crit}

Imperfection Model Number	Wave Number, k							
	1	2	4	6	8	10	12	14
73	0.74368	0.71611	0.68370	0.66390	0.64494	0.63297	0.63181	0.64640
74	0.87882	0.87435	0.86923	0.86478	0.85566	0.84236	0.83104	0.83040
75	0.94681	0.94797	0.94900	0.95011	0.94708	0.93974	0.93014	0.92391
76	0.74368	0.77045	0.79063	0.80053	0.79986	0.79654	0.79451	0.80224
77	0.87882	0.90037	0.91637	0.92422	0.92456	0.92007	0.91316	0.91040
78	0.94681	0.95953	0.96789	0.97310	0.97342	0.97101	0.96635	0.96093
79	0.74368	0.81556	0.86425	0.88611	0.89326	0.89466	0.89258	0.89474
80	0.87882	0.92134	0.94697	0.95846	0.96165	0.96108	0.95754	0.95385
81	0.94681	0.96877	0.97993	0.98596	0.98696	0.98637	0.98443	0.98047
82	0.88053	0.86504	0.84619	0.83348	0.81537	0.79709	0.78282	0.78285
83	0.93789	0.93243	0.92667	0.92279	0.91209	0.89546	0.87525	0.86582
84	0.96528	0.96198	0.95872	0.95714	0.94871	0.93337	0.91020	0.89528
85	0.88053	0.88887	0.89373	0.89565	0.88825	0.87587	0.86038	0.85511
86	0.93789	0.94297	0.94576	0.94691	0.93996	0.92615	0.90484	0.89166
87	0.96528	0.96655	0.96614	0.96610	0.95872	0.94441	0.92055	0.90384
88	0.88053	0.90808	0.92462	0.93154	0.92751	0.91647	0.89798	0.88719
89	0.93789	0.95140	0.95791	0.96041	0.95428	0.94098	0.91818	0.90236
90	0.96528	0.97017	0.97083	0.97106	0.96378	0.94962	0.92511	0.90736

TABLE III (Cont'd)

Buckling Loads, λ_{crit}

Imperfection Model Number	Wave Number, k							
	1	2	4	6	8	10	12	14
91	0.82030	0.79942	0.77450	0.75800	0.73820	0.721[illegible]	0.71278	0.71938
92	0.90841	0.90276	0.89691	0.89208	0.88059	0.86360	0.84591	0.84032
93	0.95129	0.94907	0.94702	0.94555	0.93711	0.92153	0.89955	0.88663
94	0.82030	0.83557	0.84619	0.85057	0.84458	0.83444	0.82364	0.82393
95	0.90841	0.91923	0.92667	0.92951	0.92347	0.91032	0.89119	0.88089
96	0.95129	0.95626	0.95872	0.95965	0.95283	0.93878	0.91582	0.90029
97	0.82030	0.86504	0.89373	0.90562	0.90420	0.89546	0.88056	0.87376
98	0.90841	0.93243	0.94576	0.95069	0.94584	0.93337	0.91208	0.89793
99	0.95129	0.96198	0.96614	0.96749	0.96081	0.[illegible]4697	0.92300	0.90590
100	0.73068	0.70225	0.67028	0.65064	0.63169	0.[illegible].990	0.61930	0.63485
101	0.86285	0.85686	0.85105	0.84516	0.83313	0.81640	0.80231	0.80172
102	0.92934	0.92878	0.92864	0.92739	0.91904	0.90322	0.88298	0.87287
103	0.73068	0.75534	0.77450	0.78308	0.78017	0.77425	0.77010	0.77762
104	0.86285	0.88225	0.89691	0.90247	0.89799	0.88607	0.87012	0.86382
105	0.92934	0.94007	0.94702	0.94949	0.94356	0.92994	0.90835	0.89458
106	0.73068	0.79942	0.84619	0.86574	0.86861	0.86360	0.85391	0.85264
107	0.86285	0.90276	0.92667	0.93542	0.93262	0.92153	0.90250	0.89085
108	0.92934	0.94907	0.95872	0.96185	0.95611	0.94279	0.91974	0.90355

TABLE III (Cont'd)

Buckling Loads, λ_{crit}

Imperfection Model Number	Wave Number, k							
	1	2	4	6	8	10	12	14
109	0.88982	0.87871	0.86208	0.85111	0.83556	0.82003	0.80766	0.80728
110	0.94794	0.94730	0.94453	0.94347	0.93788	0.92890	0.91758	0.91096
111	0.97567	0.97742	0.97738	0.97910	0.97705	0.97280	0.96565	0.95729
112	0.88982	0.90297	0.91078	0.91537	0.91253	0.90675	0.89871	0.89610
113	0.94794	0.95806	0.96410	0.96848	0.96765	0.96430	0.95781	0.95104
114	0.97567	0.98207	0.98499	0.98839	0.98780	0.98589	0.98153	0.97334
115	0.88982	0.92253	0.94244	0.95255	0.95435	0.95303	0.94806	0.94350
116	0.94794	0.96664	0.97656	0.98248	0.98302	0.98178	0.97778	0.97048
117	0.97567	0.98576	0.98980	0.99354	0.99324	0.99211	0.98896	0.98024
118	0.82883	0.81187	0.78869	0.77326	0.75477	0.73923	0.73069	0.73645
119	0.91809	0.91711	0.91404	0.91168	0.90439	0.89302	0.88093	0.87661
120	0.96149	0.96427	0.96539	0.96707	0.96461	0.95891	0.95022	0.94257
121	0.82883	0.84870	0.86208	0.86876	0.86632	0.86075	0.85441	0.85600
122	0.91809	0.93388	0.94453	0.95045	0.95003	0.94593	0.93870	0.93340
123	0.96149	0.97159	0.97738	0.98170	0.98146	0.97917	0.97410	0.96650
124	0.82883	0.87871	0.91078	0.92569	0.92949	0.92890	0.92449	0.92252
125	0.91809	0.94730	0.96410	0.97240	0.97396	0.97280	0.96846	0.96208
126	0.96149	0.97742	0.98499	0.98984	0.99004	0.98892	0.98556	0.97741

TABLE III (Cont'd)

Buckling Loads, λ_{crit}

Imperfection Model Number	Wave Number, k							
	1	2	4	6	8	10	12	14
127	0.73804	0.71294	0.68209	0.66282	0.64411	0.63232	0.63128	0.64598
128	0.87192	0.87035	0.86706	0.86317	0.85425	0.84101	0.82974	0.82925
129	0.93925	0.94359	0.94656	0.94825	0.94530	0.93776	0.92767	0.92120
130	0.73804	0.76699	0.78869	0.79910	0.79863	0.79539	0.79343	0.80128
131	0.87192	0.89623	0.91404	0.92244	0.92288	0.91825	0.91099	0.90811
132	0.93925	0.95508	0.96539	0.97116	0.97152	0.96874	0.96294	0.95615
133	0.73804	0.81187	0.86208	0.88444	0.89171	0.89302	0.89070	0.89278
134	0.87192	0.91711	0.94453	0.95657	0.95980	0.95891	0.95442	0.94962
135	0.93925	0.96427	0.97738	0.98398	0.98499	0.98393	0.98027	0.97281
136	0.89454	0.88215	0.86410	0.85261	0.83687	0.82125	0.80880	0.80826
137	0.95302	0.95108	0.94680	0.94524	0.93957	0.93075	0.91980	0.91331
138	0.98093	0.98133	0.97976	0.98097	0.97891	0.97505	0.96908	0.96222
139	0.89454	0.90655	0.91295	0.91706	0.91411	0.90844	0.90065	0.89808
140	0.95302	0.96188	0.96643	0.97032	0.96948	0.96647	0.96098	0.95525
141	0.98093	0.98601	0.98739	0.99030	0.98972	0.98828	0.98564	0.98097
142	0.89454	0.92619	0.94470	0.95435	0.95611	0.95509	0.95094	0.94721
143	0.95302	0.97050	0.97894	0.98437	0.98492	0.98413	0.98171	0.97729
144	0.98093	0.98971	0.99222	0.99546	0.99519	0.99458	0.99353	0.99050

TABLE III (Cont'd)

Buckling Loads, λ_{crit}

Imperfection Model Number	Wave Number, k							
	1	2	4	6	8	10	12	14
145	0.83313	0.81503	0.79050	0.77456	0.75584	0.74015	0.73148	0.73711
146	0.92298	0.92073	0.91622	0.91336	0.90595	0.89462	0.88265	0.87825
147	0.96666	0.96812	0.96773	0.96891	0.96642	0.96103	0.95315	0.94623
148	0.83313	0.85203	0.86410	0.87031	0.86773	0.86217	0.85587	0.85739
149	0.92298	0.93759	0.94680	0.95224	0.95177	0.94792	0.94134	0.93655
150	0.96666	0.97548	0.97976	0.98359	0.98335	0.98149	0.97793	0.97267
151	0.83313	0.88215	0.91295	0.92741	0.93115	0.93075	0.92684	0.92523
152	0.92298	0.95108	0.96643	0.97425	0.97581	0.97505	0.97199	0.96760
153	0.96666	0.98133	0.98739	0.99175	0.99197	0.99135	0.98991	0.98632
154	0.74179	0.71566	0.68359	0.66386	0.64491	0.63296	0.63180	0.64639
155	0.87653	0.87378	0.86909	0.86471	0.85562	0.84232	0.83101	0.83038
156	0.94428	0.94734	0.94884	0.95003	0.94702	0.93969	0.93008	0.92386
157	0.74179	0.76995	0.79050	0.80047	0.79982	0.79651	0.79449	0.80222
158	0.87653	0.89978	0.91622	0.92414	0.92451	0.92002	0.91311	0.91036
159	0.94428	0.95889	0.96773	0.97302	0.97336	0.97095	0.96628	0.96083
160	0.74179	0.81503	0.86410	0.88603	0.89321	0.89462	0.89254	0.89470
161	0.87653	0.92073	0.94680	0.95838	0.96159	0.96103	0.95747	0.95377
162	0.94428	0.96812	0.97976	0.98588	0.98690	0.98631	0.98434	0.98029

TABLE III (Cont'd)

Buckling Loads, λ_{crit}

Imperfection Model Number	Wave Number, k							
	1	2	4	6	8	10	12	14
163	0.86237	0.84728	0.82858	0.81506	0.79525	0.77542	0.76070	0.76188
164	0.91830	0.91307	0.90691	0.90126	0.88684	0.86576	0.84301	0.83497
165	0.94499	0.94192	0.93808	0.93434	0.92123	0.89972	0.87284	0.86013
166	0.86237	0.87054	0.87486	0.87509	0.86436	0.84801	0.83006	0.82575
167	0.91830	0.92336	0.92548	0.92448	0.91303	0.89329	0.86832	0.85706
168	0.94499	0.94638	0.94529	0.94296	0.93060	0.90949	0.88154	0.86743
169	0.86237	0.88929	0.90491	0.90970	0.90135	0.88466	0.86250	0.85324
170	0.91830	0.93159	0.93730	0.93748	0.92644	0.90645	0.87954	0.86617
171	0.94499	0.94991	0.94985	0.94773	0.93532	0.91407	0.88534	0.87044
172	0.80363	0.78320	0.75876	0.74199	0.72152	0.70452	0.69597	0.70367
173	0.88956	0.88410	0.87795	0.87165	0.85712	0.83682	0.81735	0.81291
174	0.93135	0.92931	0.92670	0.92318	0.91035	0.88918	0.86383	0.85274
175	0.80363	0.81853	0.82858	0.83157	0.82301	0.81005	0.79757	0.79856
176	0.88956	0.90018	0.90691	0.90774	0.89755	0.87914	0.85671	0.84787
177	0.93135	0.93633	0.93808	0.93675	0.92508	0.90450	0.87756	0.86440
178	0.80363	0.84728	0.87486	0.88470	0.87942	0.86576	0.84756	0.84178
179	0.88956	0.91307	0.92548	0.92813	0.91853	0.89972	0.87442	0.86238
180	0.93135	0.94192	0.94529	0.94430	0.93255	0.91173	0.88361	0.86919

TABLE III (Cont'd)

Buckling Loads, λ_{crit}

Imperfection Model Number	Wave Number, k							
	1	2	4	6	8	10	12	14
181	0.71628	0.68833	0.65718	0.60500	0.61904	0.60756	0.60762	0.62412
182	0.84513	0.83929	0.83331	0.82634	0.81214	0.79337	0.77840	0.77884
183	0.90994	0.90950	0.90882	0.90569	0.89339	0.87276	0.84966	0.84101
184	0.71628	0.74018	0.75876	0.76629	0.76168	0.75407	0.74907	0.75715
185	0.84513	0.86410	0.87795	0.88167	0.87356	0.85728	0.83855	0.83326
186	0.90994	0.92052	0.92670	0.92698	0.91640	0.89666	0.87128	0.85055
187	0.71628	0.78320	0.82858	0.84622	0.84580	0.83682	0.82438	0.82362
188	0.84513	0.88410	0.90691	0.91343	0.90614	0.88918	0.86630	0.85635
189	0.90994	0.92931	0.93808	0.93887	0.92815	0.90804	0.88086	0.86720
190	0.88053	0.87412	0.85978	0.84948	0.83417	0.81875	0.80646	0.80627
191	0.93789	0.94232	0.94195	0.94155	0.93609	0.92697	0.91532	0.90863
192	0.96528	0.97224	0.97468	0.97706	0.97507	0.97046	0.96221	0.95299
193	0.88053	0.89824	0.90831	0.91354	0.91084	0.90498	0.89672	0.89410
194	0.93789	0.95299	0.96144	0.96647	0.96572	0.96205	0.95466	0.94712
195	0.96528	0.97686	0.98226	0.98632	0.98577	0.98340	0.97753	0.96744
196	0.88053	0.91767	0.93986	0.95060	0.95248	0.95089	0.94517	0.94000
197	0.93789	0.96152	0.97386	0.98043	0.98102	0.97935	0.97395	0.96496
198	0.96528	0.98052	0.98706	0.99145	0.99118	0.98955	0.98460	0.97363

TABLE III (Cont'd)

Buckling Loads, λ_{crit}

Imperfection Model Number	Wave Number, k							
	1	2	4	6	8	10	12	14
199	0.82030	0.80768	0.78664	0.77184	0.75363	0.73827	0.72987	0.73578
200	0.90841	0.91229	0.91156	0.90987	0.90275	0.89135	0.87916	0.87494
201	0.95129	0.95917	0.96273	0.96507	0.96269	0.95672	0.94729	0.93908
202	0.82030	0.84430	0.85978	0.86707	0.86482	0.85927	0.85290	0.85459
203	0.90841	0.92896	0.94195	0.94850	0.94818	0.94385	0.93603	0.93035
204	0.95129	0.96644	0.97468	0.97965	0.97946	0.97676	0.97041	0.96140
205	0.82030	0.87412	0.90831	0.92383	0.92774	0.92697	0.92207	0.91986
206	0.90841	0.94232	0.96144	0.97038	0.97200	0.97046	0.96496	0.95740
207	0.95129	0.97224	0.98226	0.98776	0.98800	0.98640	0.98131	0.97102
208	0.73068	0.70934	0.68038	0.66170	0.64327	0.63165	0.63074	0.64555
209	0.86285	0.86583	0.86474	0.86150	0.85279	0.83963	0.82842	0.82808
210	0.92934	0.93863	0.94397	0.94631	0.94348	0.93576	0.92523	0.91853
211	0.73068	0.76307	0.78664	0.79762	0.79736	0.79423	0.79233	0.80030
212	0.86285	0.89154	0.91156	0.92058	0.92115	0.91640	0.90883	0.90587
213	0.92934	0.95003	0.96273	0.96915	0.96957	0.96645	0.95962	0.95189
214	0.73068	0.80768	0.85978	0.88271	0.89011	0.89135	0.88878	0.89082
215	0.86285	0.91229	0.94195	0.95460	0.95791	0.95672	0.95137	0.94577
216	0.92934	0.95917	0.97468	0.98193	0.98297	0.98148	0.97632	0.96700

TABLE III (Cont'd)

Buckling Loads, λ_{crit}

Imperfection Model Number	Wave Number, k							
	1	2	4	6	8	10	12	14
217	0.88982	0.88101	0.86381	0.85248	0.83678	0.82119	0.80875	0.80822
218	0.94794	0.94982	0.94648	0.94508	0.93946	0.93066	0.91970	0.91322
219	0.97567	0.98003	0.97942	0.98080	0.97879	0.97493	0.96893	0.96202
220	0.88982	0.90535	0.91263	0.91690	0.91400	0.90835	0.90057	0.89800
221	0.94794	0.96061	0.96610	0.97016	0.96936	0.96635	0.96084	0.95508
222	0.97567	0.98469	0.98705	0.99013	0.98959	0.98816	0.98546	0.98062
223	0.88982	0.92497	0.94438	0.95418	0.95599	0.95498	0.95082	0.94707
224	0.94794	0.96921	0.97860	0.98420	0.98479	0.98401	0.98153	0.97700
225	0.97567	0.98839	0.99187	0.99529	0.99506	0.99445	0.99332	0.98994
226	0.82883	0.81397	0.79024	0.77444	0.75576	0.74011	0.73145	0.73708
227	0.91809	0.91952	0.91591	0.91320	0.90584	0.89454	0.88258	0.87819
228	0.96149	0.96684	0.96739	0.96874	0.96630	0.96092	0.95302	0.94609
229	0.82883	0.85092	0.86381	0.87017	0.86764	0.86210	0.85580	0.85734
230	0.91809	0.93635	0.94648	0.95207	0.95165	0.94782	0.94123	0.93643
231	0.96149	0.97418	0.97942	0.98342	0.98323	0.98136	0.97777	0.97225
232	0.82883	0.88101	0.91263	0.92725	0.93104	0.93066	0.92674	0.92512
233	0.91809	0.94982	0.96610	0.97408	0.97569	0.97493	0.97183	0.96737
234	0.96149	0.98003	0.98705	0.99158	0.99184	0.99122	0.98971	0.98588

TABLE III (Cont'd)

Buckling Loads, λ_{crit}

Imperfection Model Number	Wave Number, k							
	1	2	4	6	8	10	12	14
235	0.73804	0.71475	0.68337	0.66376	0.64486	0.63292	0.63178	0.64638
236	0.87192	0.87263	0.86880	0.86457	0.85553	0.84225	0.83096	0.83034
237	0.93925	0.94609	0.94851	0.94987	0.94691	0.93959	0.92998	0.92376
238	0.73804	0.76896	0.79024	0.80034	0.79974	0.79645	0.79444	0.80219
239	0.87192	0.89859	0.91591	0.92399	0.92440	0.91993	0.91302	0.91027
240	0.93925	0.95762	0.96739	0.97285	0.97324	0.97084	0.96613	0.96065
241	0.73804	0.81397	0.86381	0.88589	0.89311	0.89454	0.89245	0.89463
242	0.87192	0.91952	0.94648	0.95822	0.96146	0.96092	0.95733	0.95361
243	0.93925	0.96684	0.97942	0.98570	0.98677	0.98618	0.98416	0.97995

Notes:

1. Underlined numbers indicate the lowest calculated buckling load for that particular imperfection model.
2. Refer to Table I for wave numbers i and ℓ corresponding to the listed k.
3. Refer to Table II for description of the imperfection model corresponding to the listed model number.

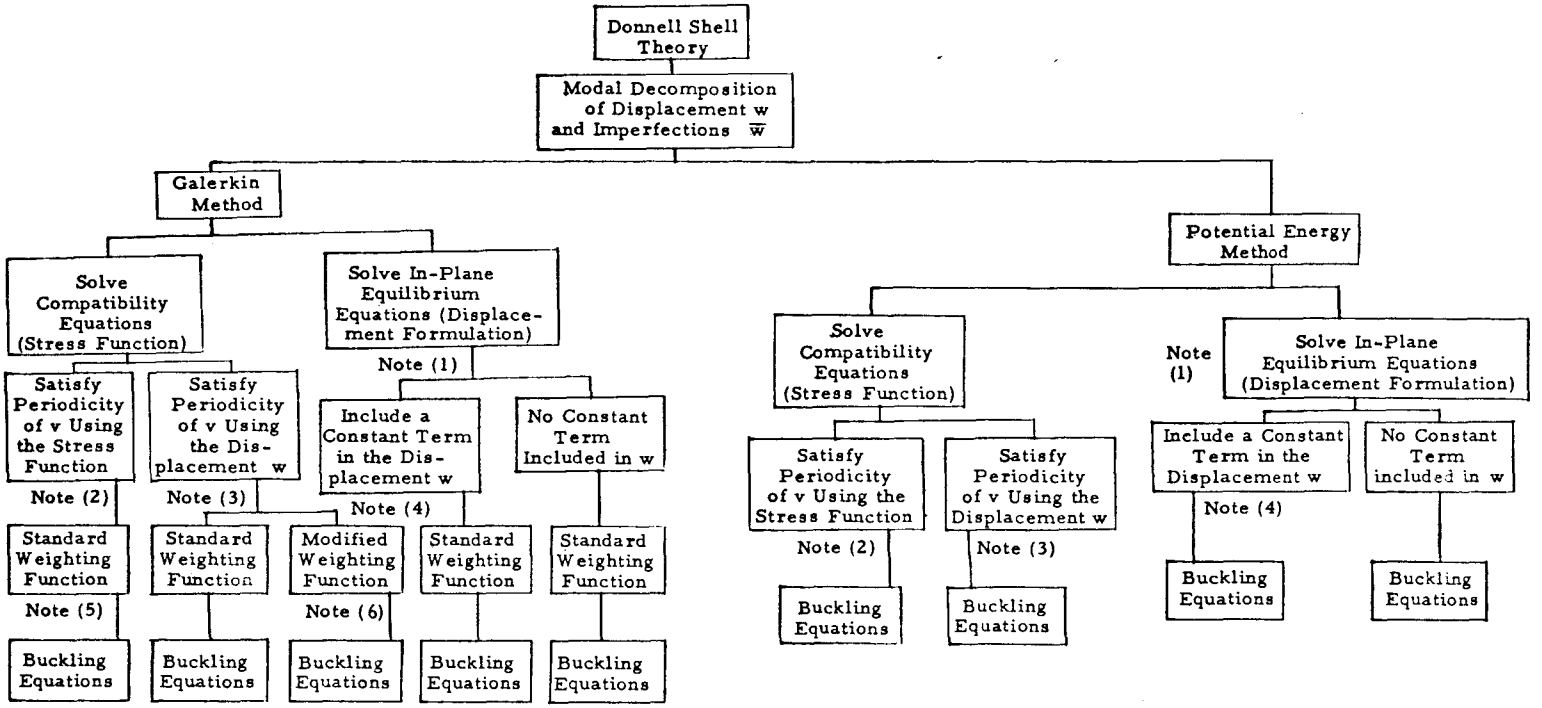

Notes:

(1) Periodicity of v automatically satisfied, i.e., $\int_0^{2\pi R} \frac{\partial v}{\partial y}\, dy = 0$

(2) $F = \frac{1}{2} Ax^2 - \frac{1}{2} \sigma t y^2 + f_p$

(3) $w = \frac{\nu \sigma R}{E}$ + (Assumed Modes) + B

(4) w = (Assumed Modes) + w_ν

(5) $\iint \mathcal{E}(x, y) \cdot$ (Assumed Mode) $dxdy = 0$

(6) $\iint \mathcal{E}(x, y) \cdot \left(\frac{\partial w}{\partial \xi_i}\right) dxdy$

Figure 1. Methods of Solution

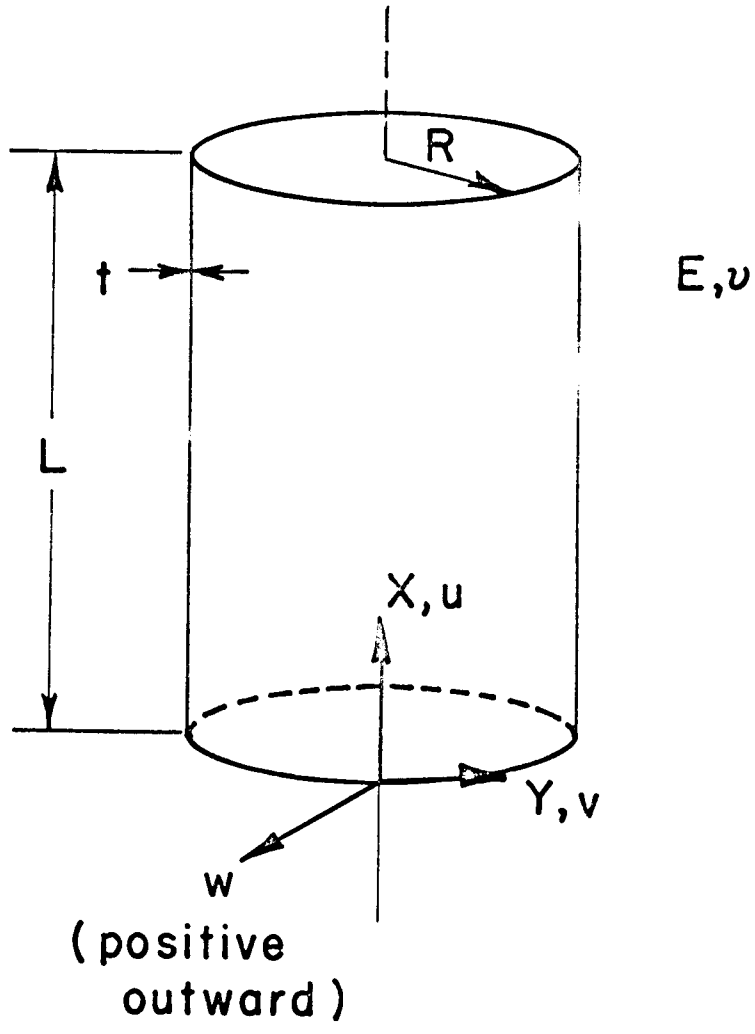

FIG. 2 SHELL COORDINATES AND GEOMETRY

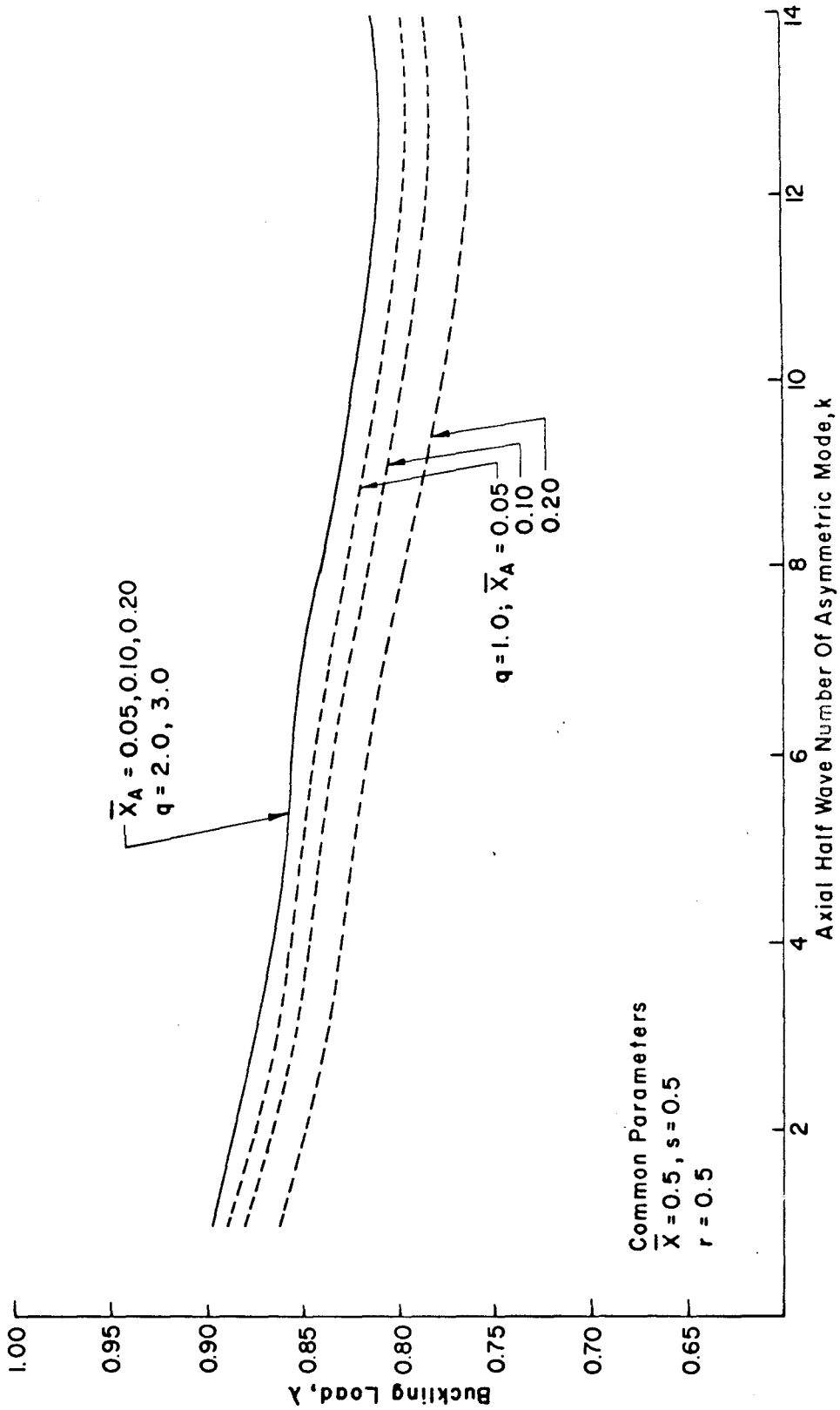

FIG. 3 COMPUTED BUCKLING LOAD

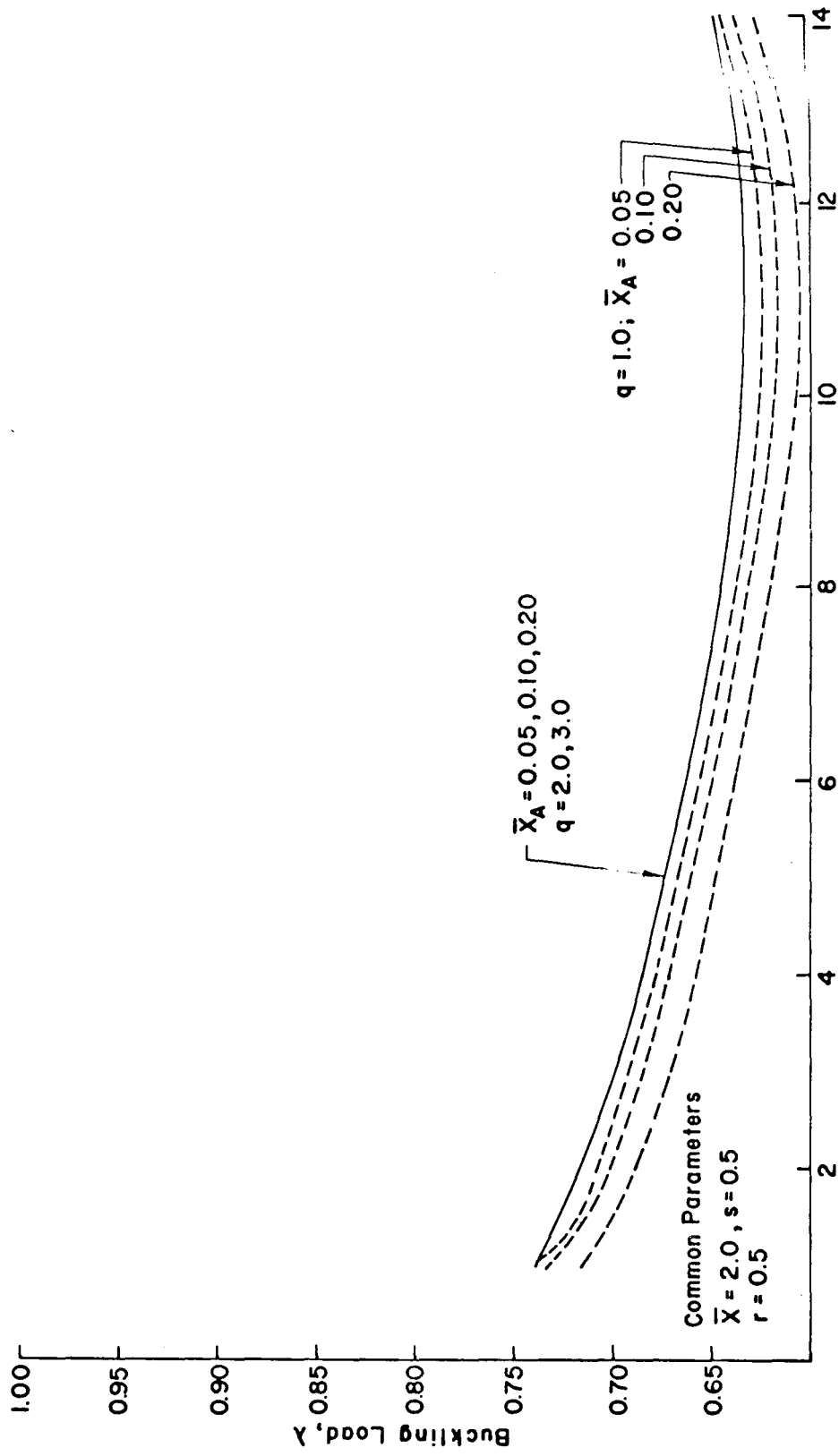

FIG. 4 COMPUTED BUCKLING LOAD

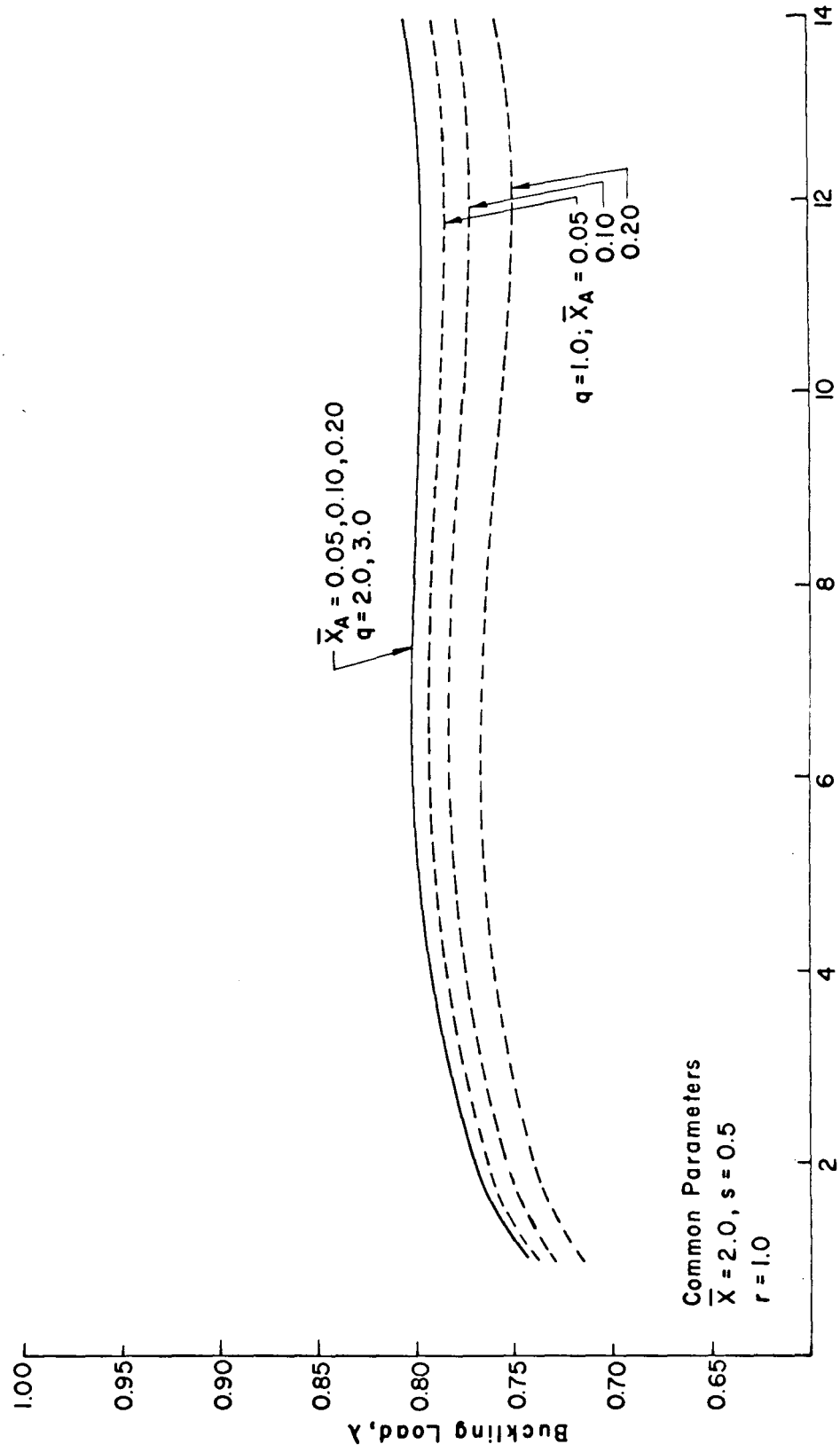

FIG. 5 COMPUTED BUCKLING LOAD

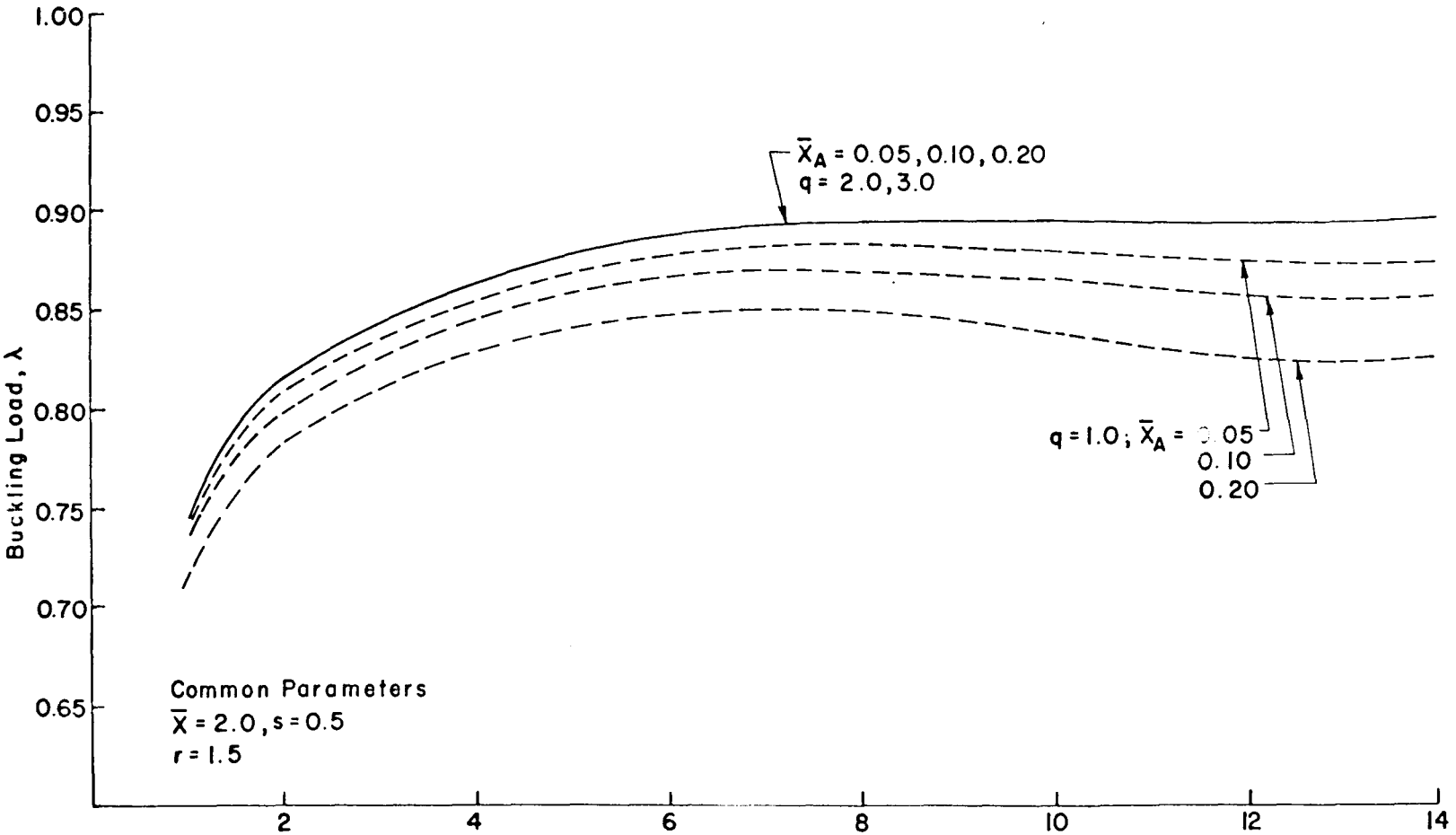

FIG. 6 COMPUTED BUCKLING LOAD

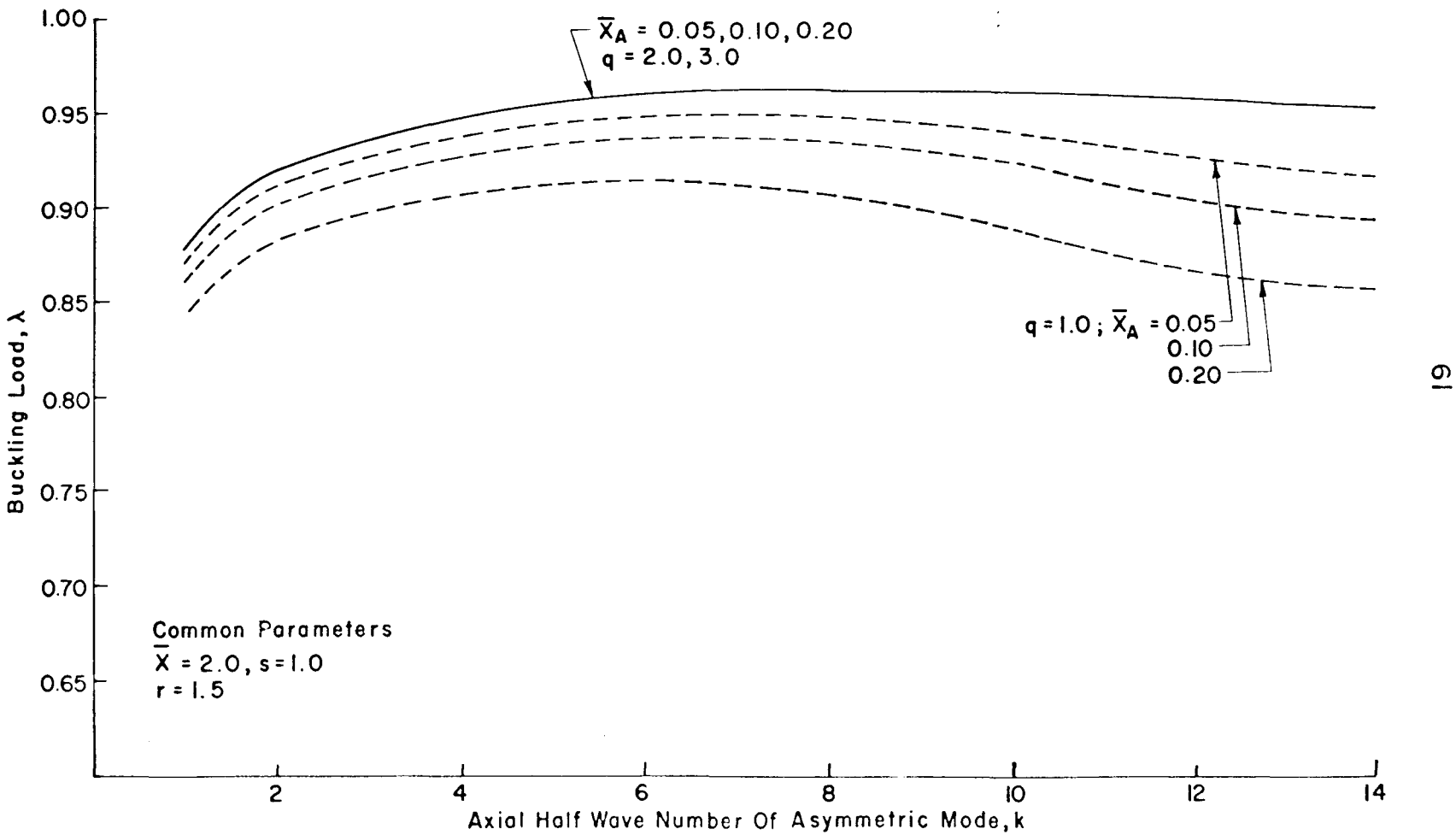

FIG. 7 COMPUTED BUCKLING LOAD

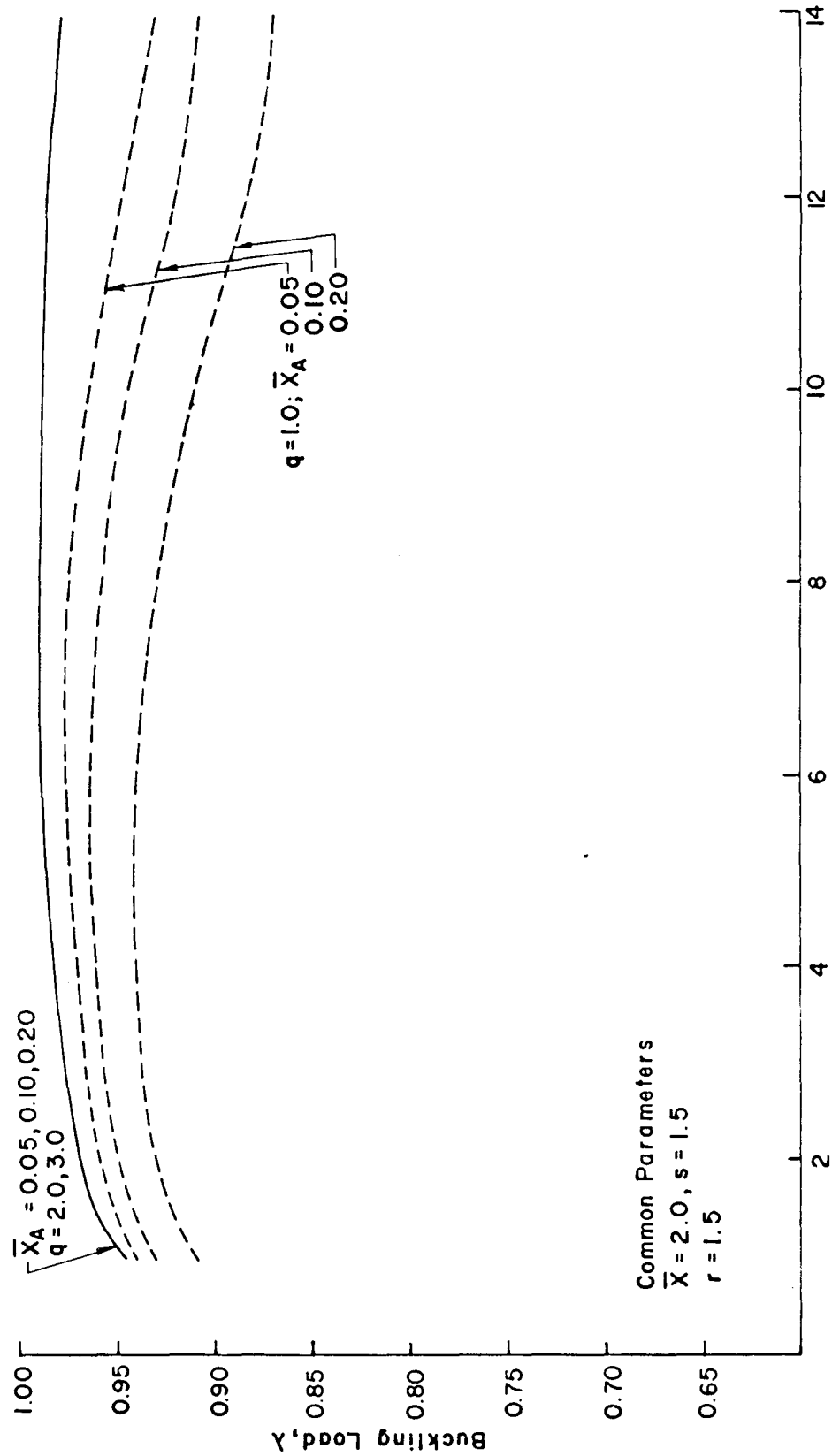

FIG. 8 COMPUTED BUCKLING LOAD

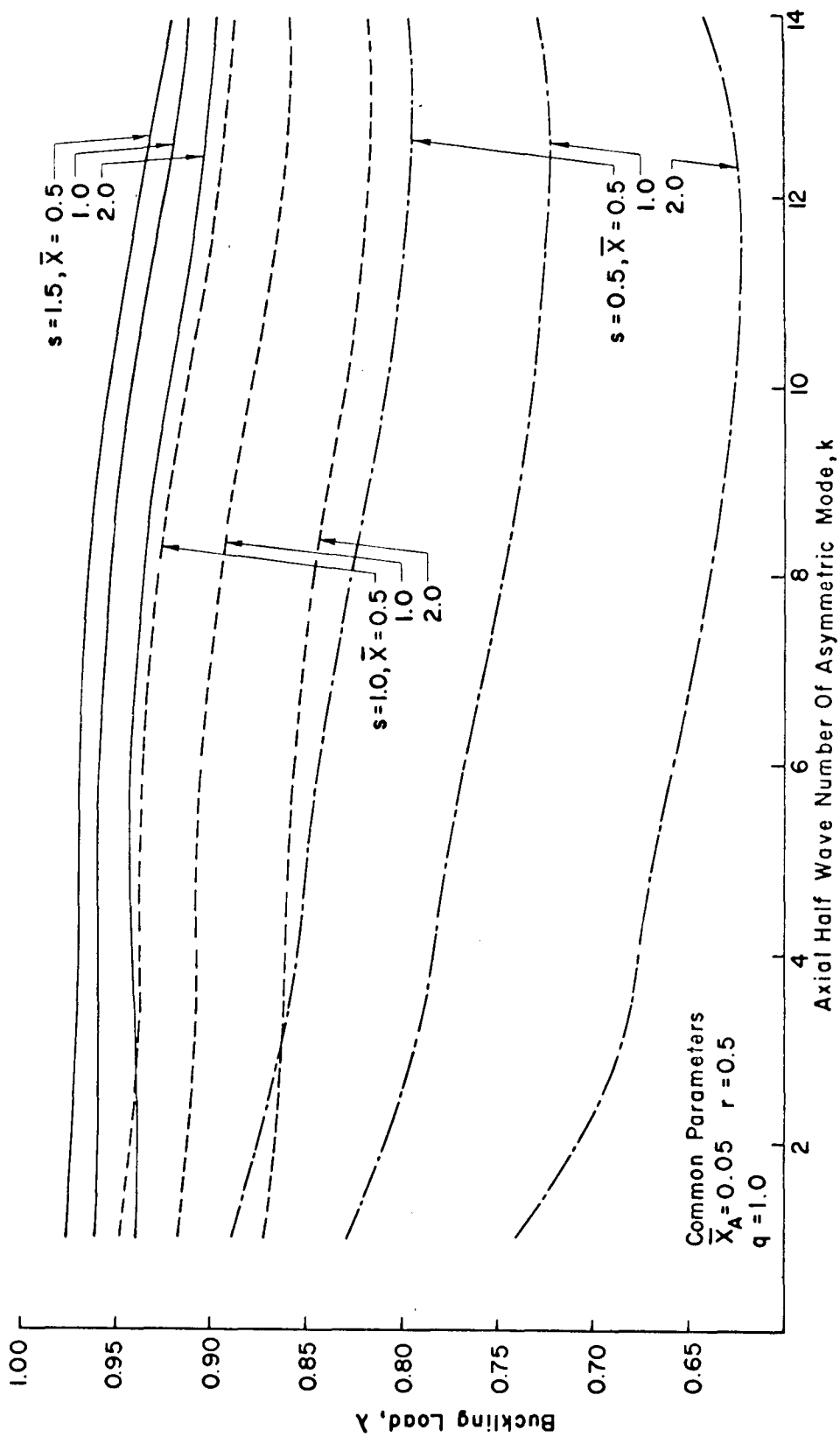

FIG. 9 COMPUTED BUCKLING LOAD

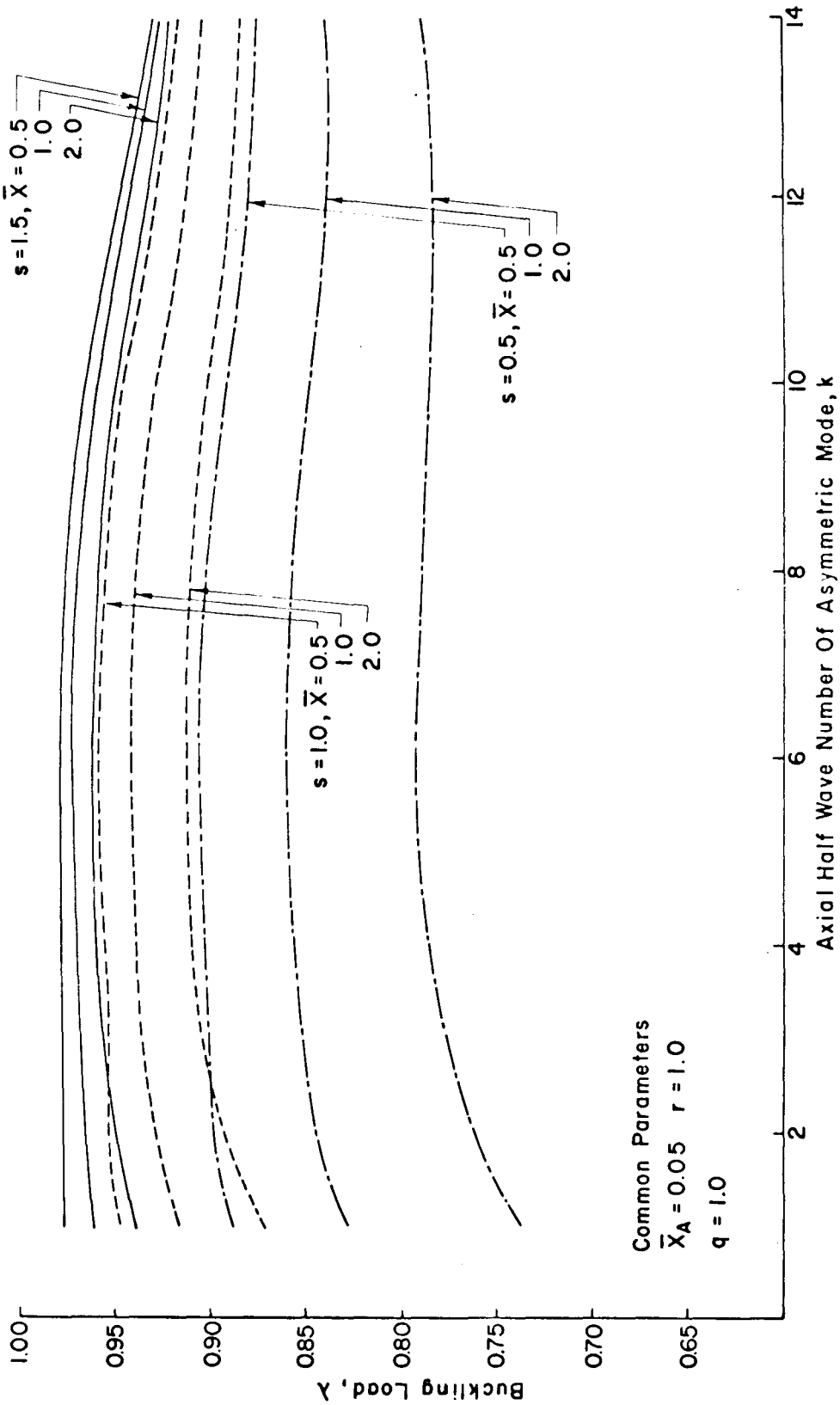

FIG. 10 COMPUTED BUCKLING LOAD

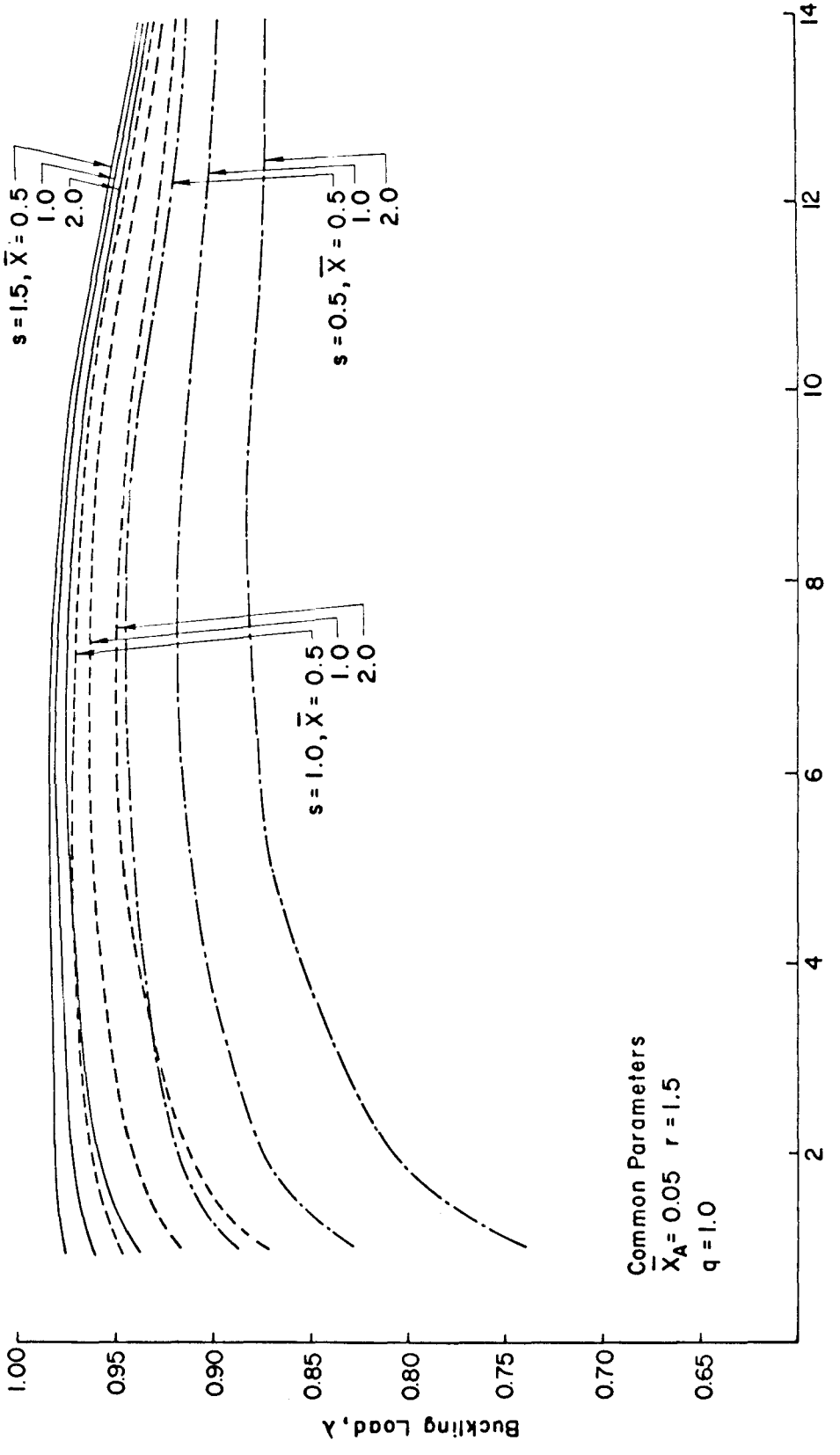

FIG.II COMPUTED BUCKLING LOAD

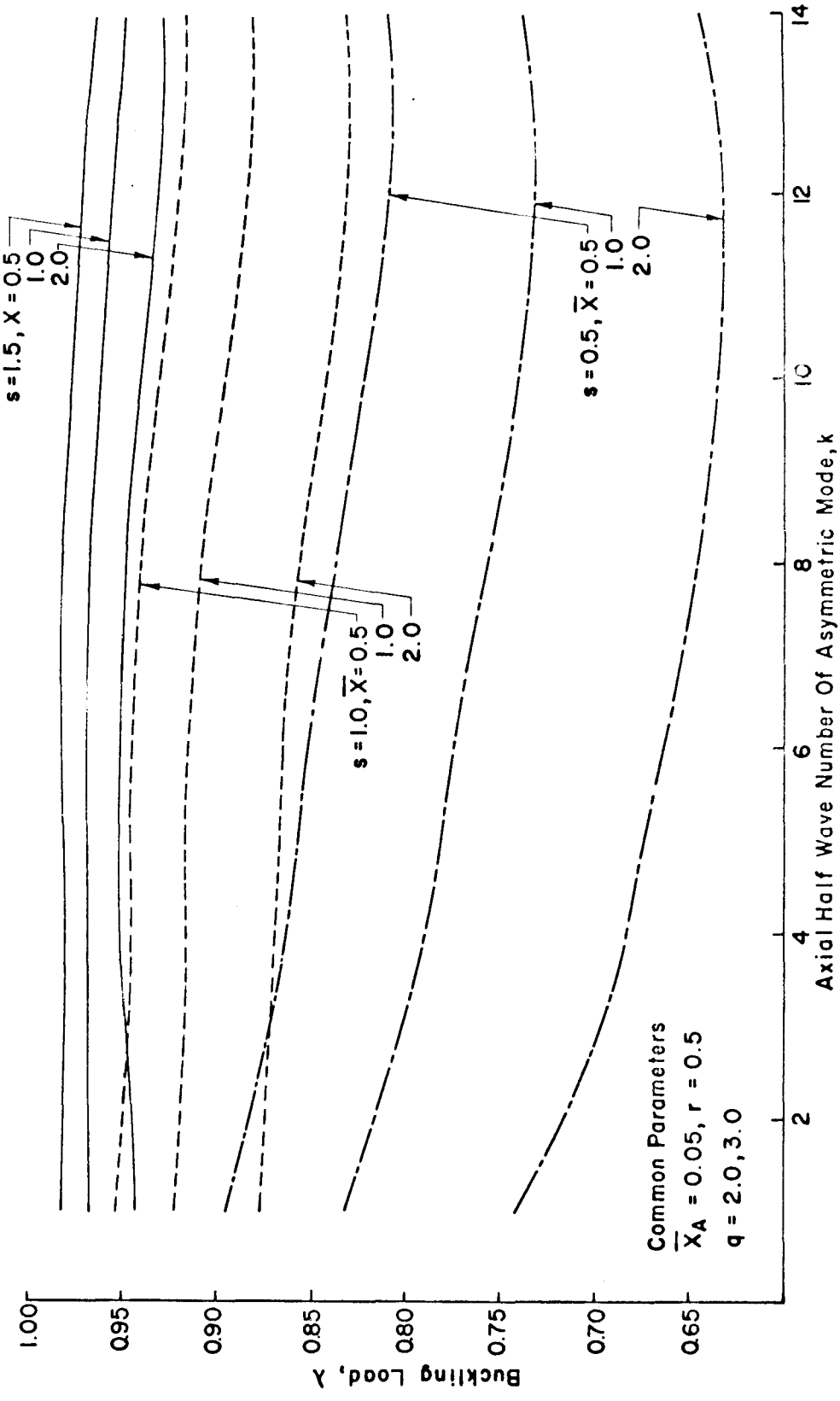

FIG.12 COMPUTED BUCKLING LOAD

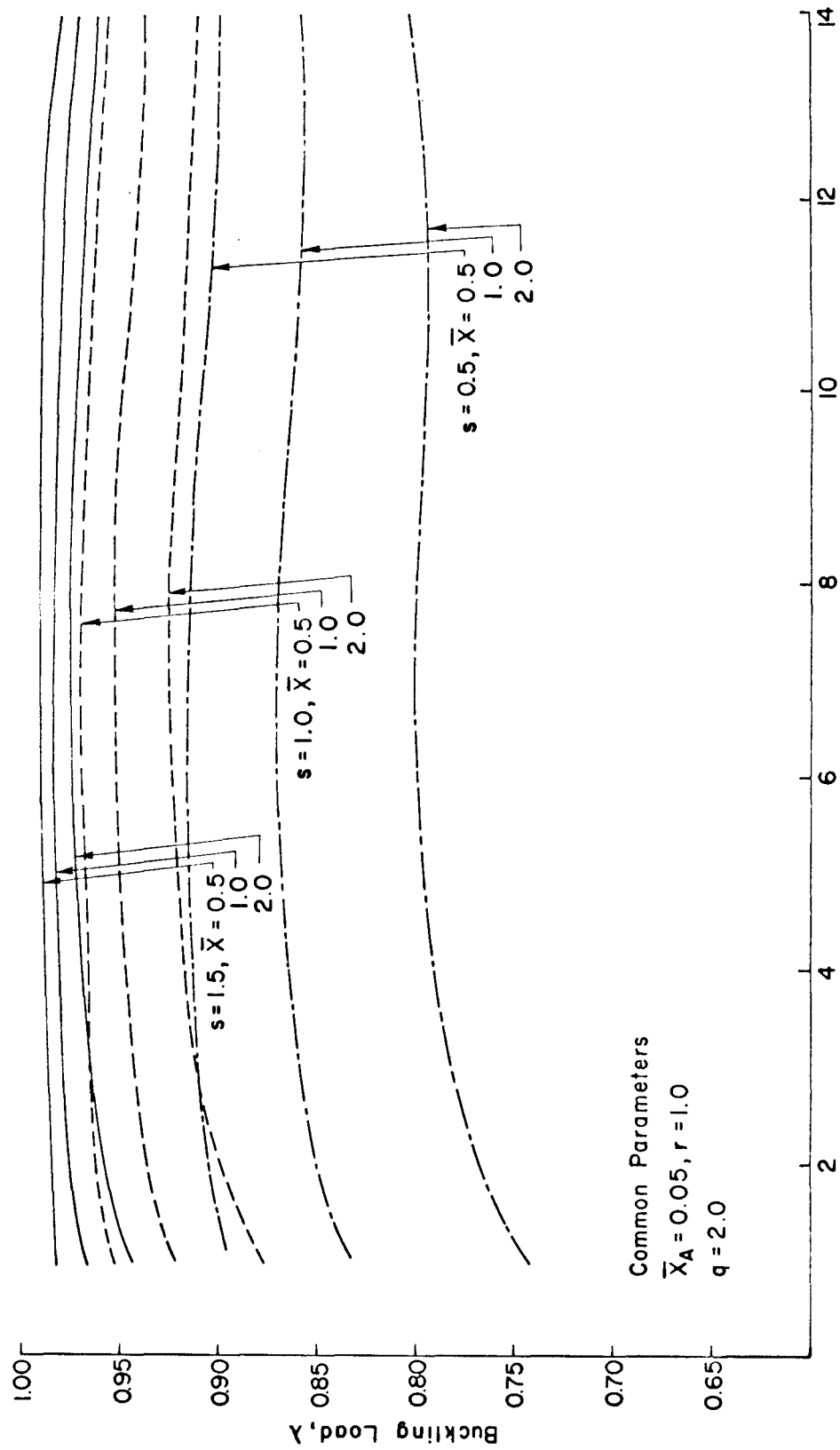

FIG. 13 COMPUTED BUCKLING LOAD

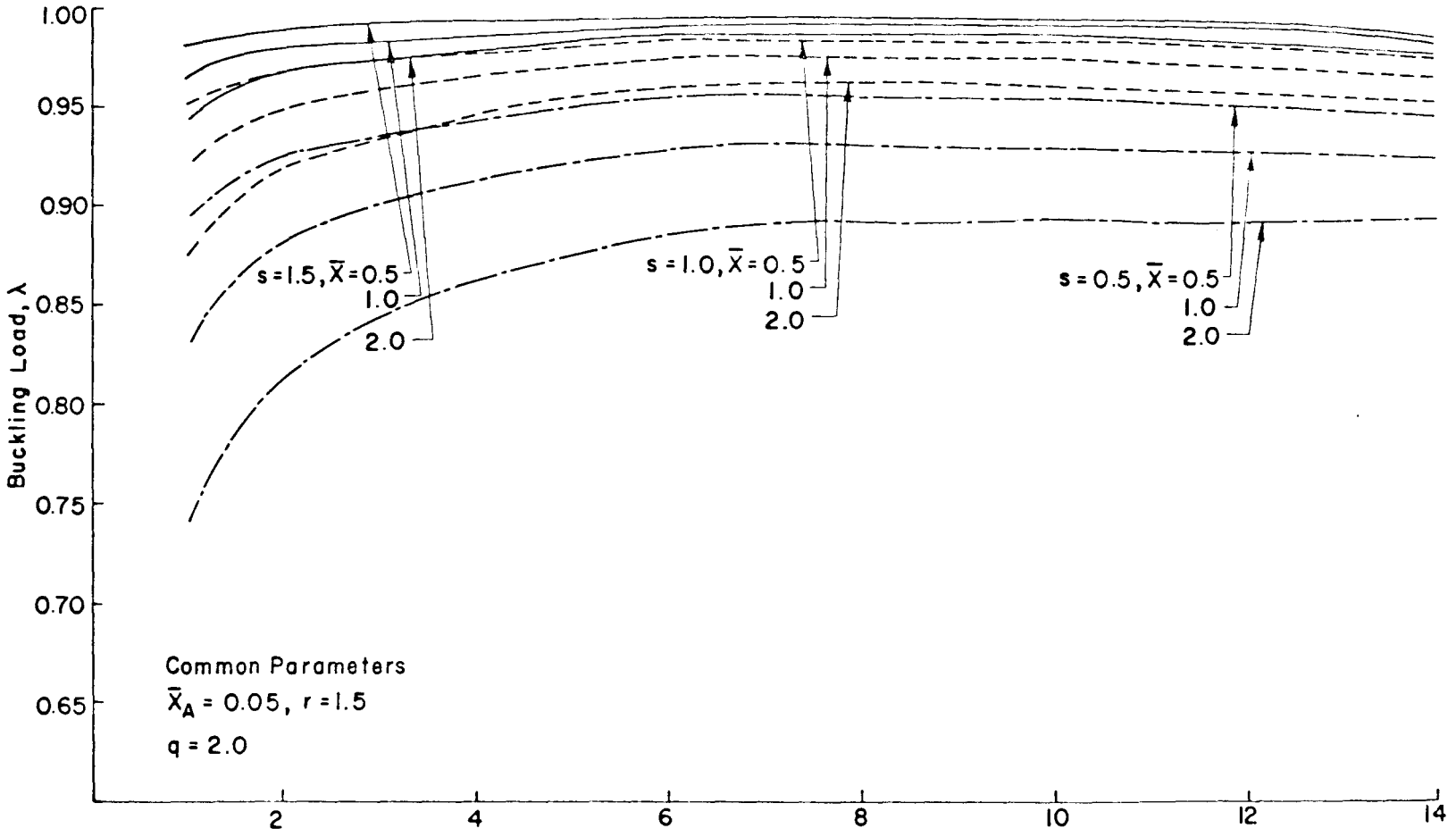

FIG. 14 COMPUTED BUCKLING LOAD

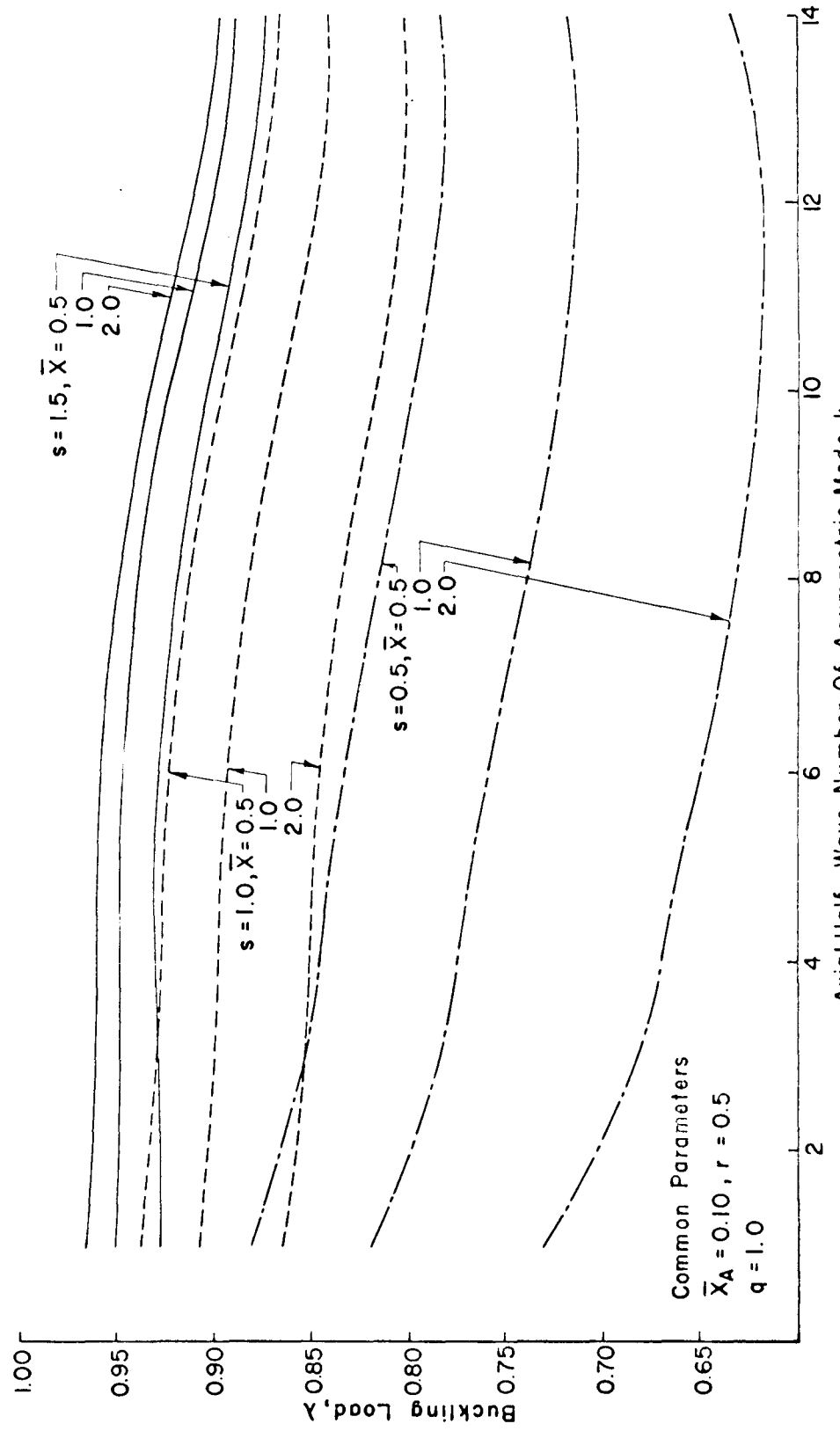

FIG. 15 COMPUTED BUCKLING LOAD

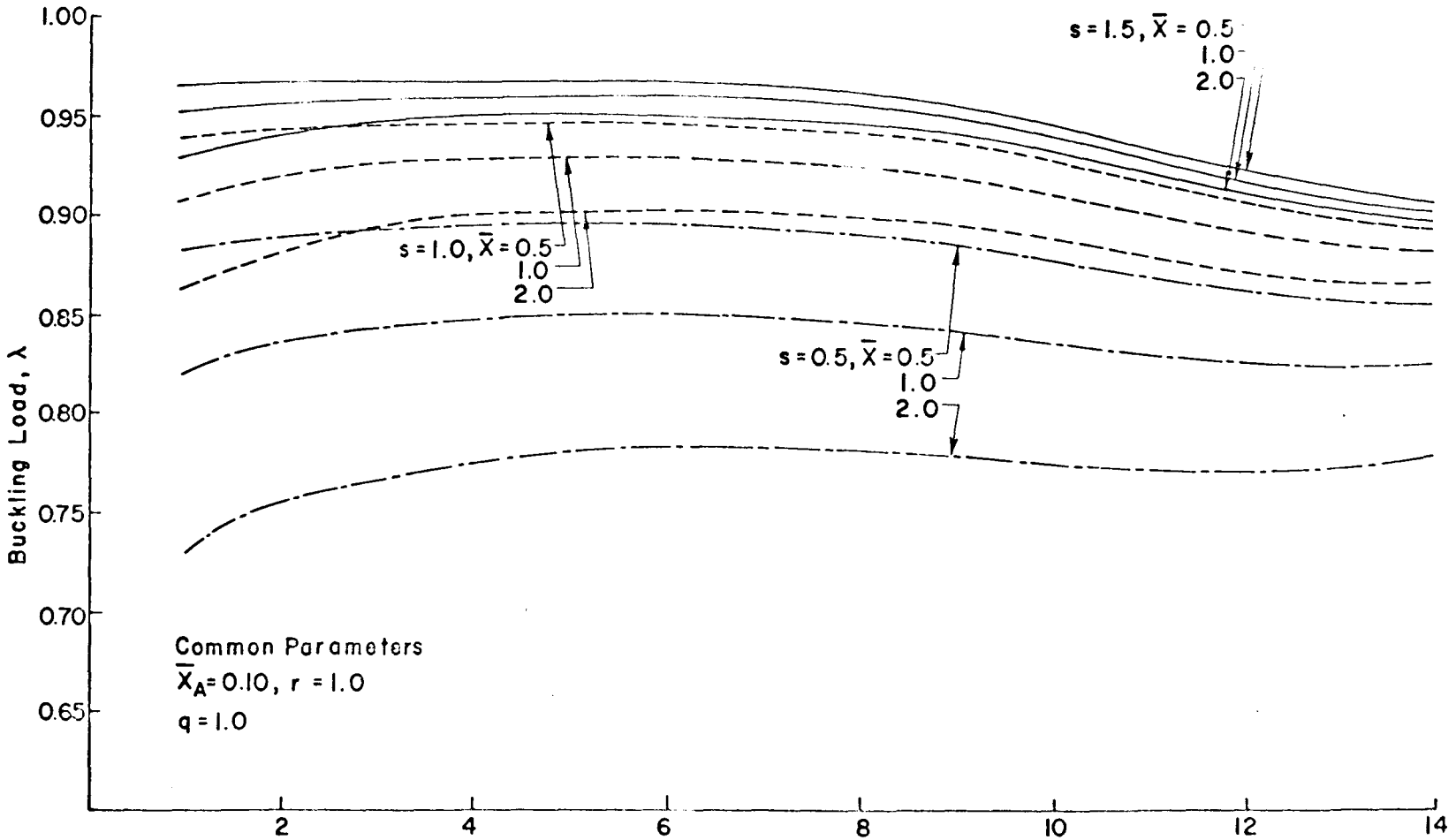

FIG. 16 COMPUTED BUCKLING LOAD

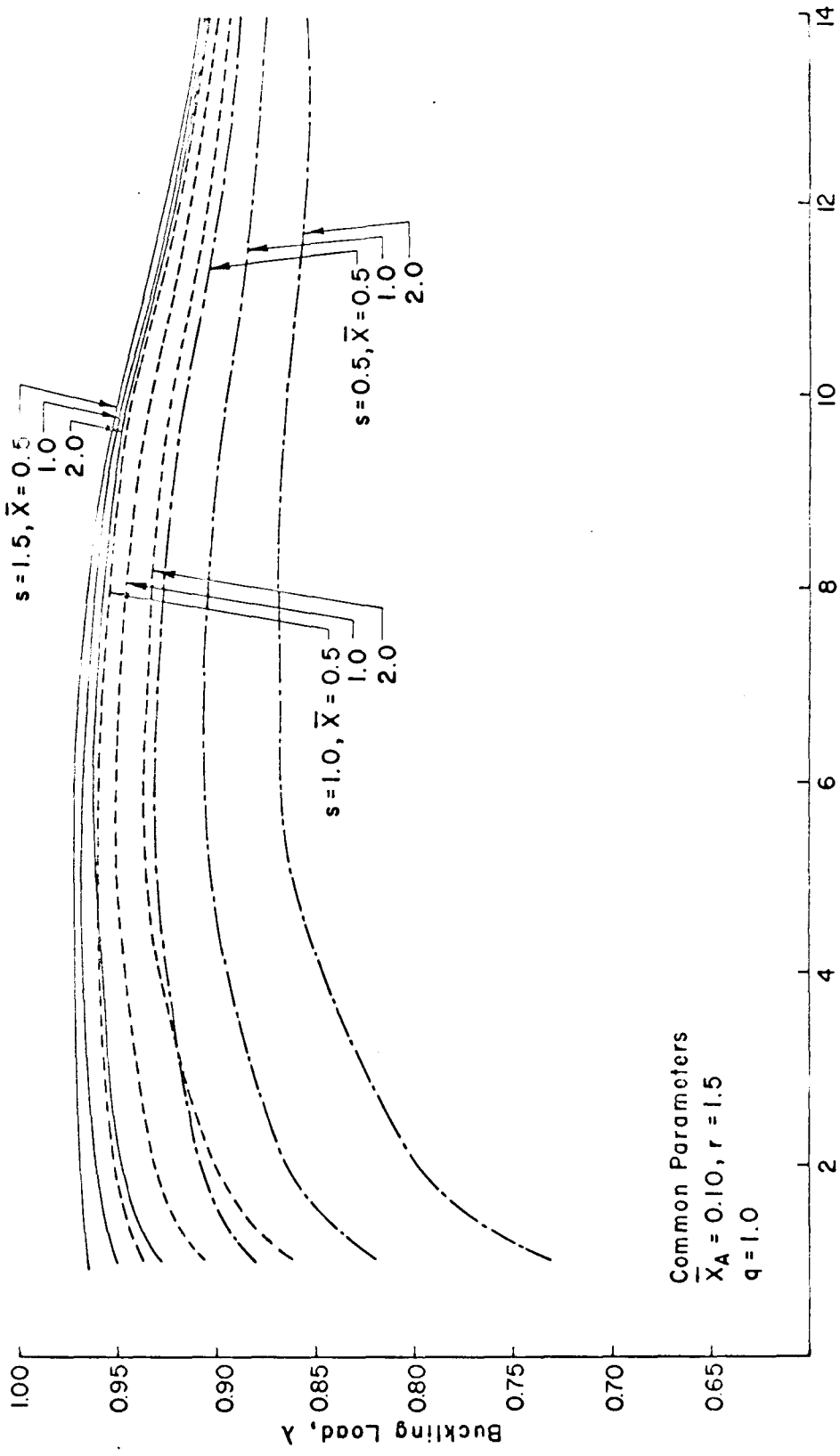

FIG.17 COMPUTED BUCKLING LOAD

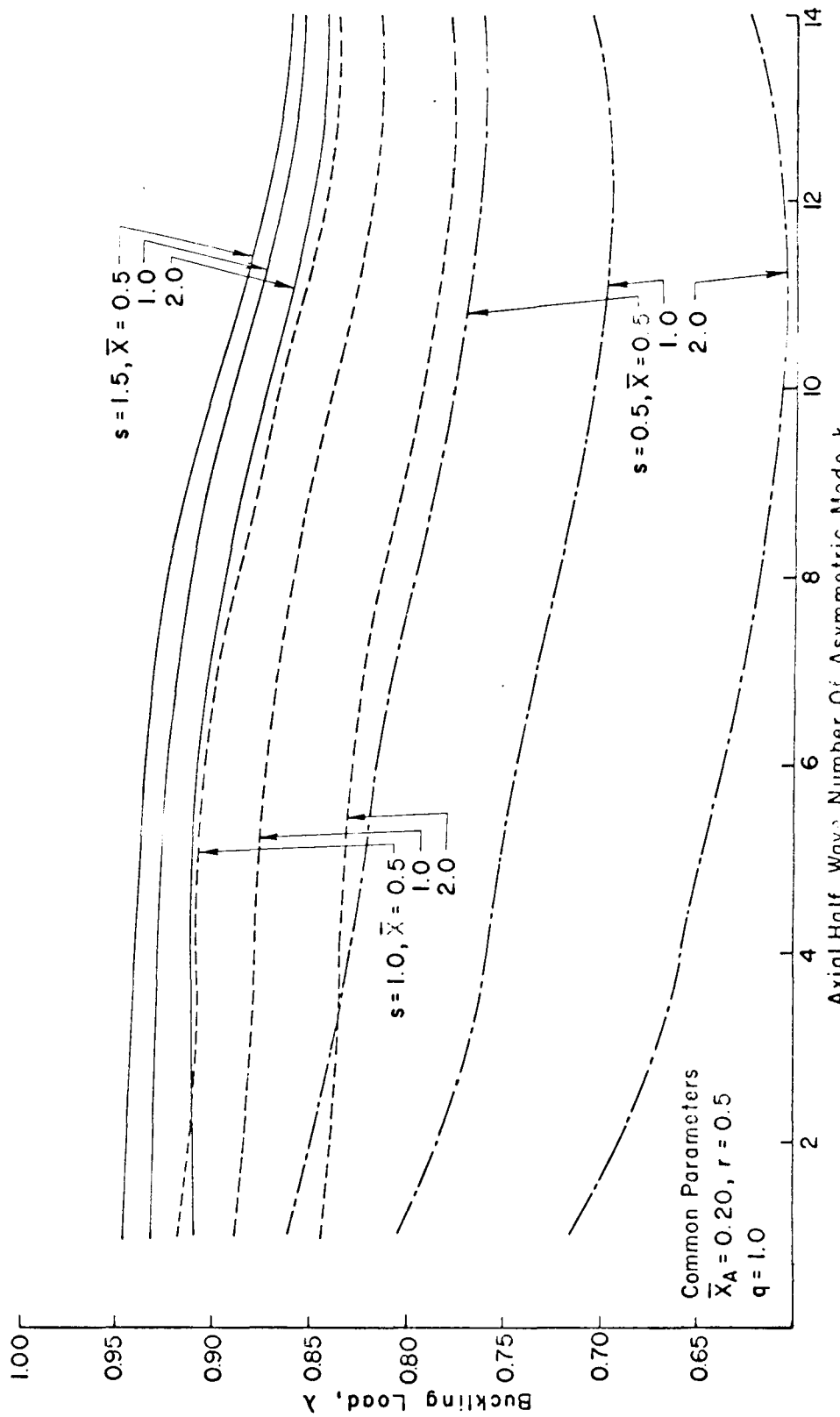

FIG.18 COMPUTED BUCKLING LOAD

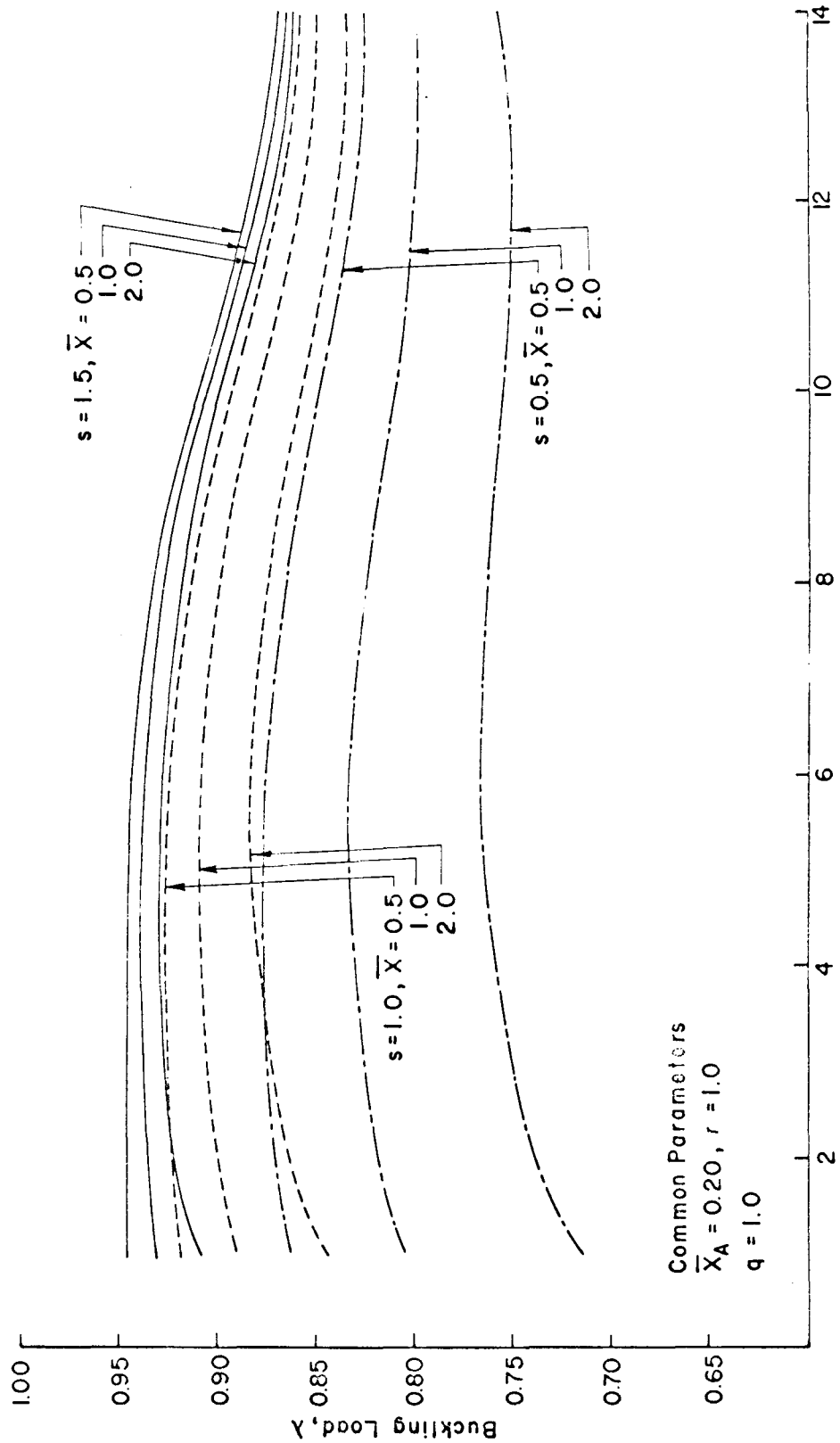

FIG. 19 COMPUTED BUCKLING LOAD

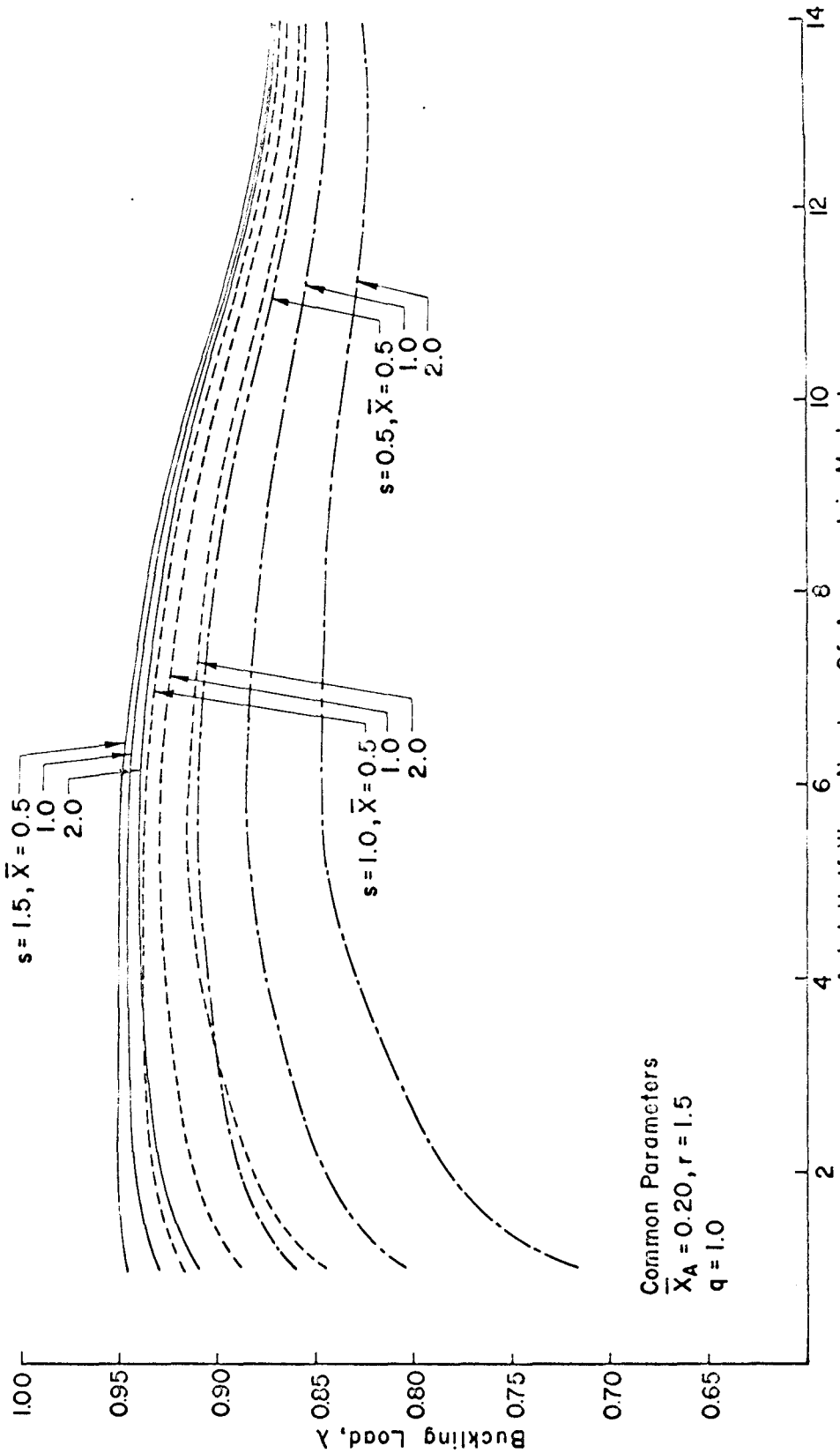

FIG. 20 COMPUTED BUCKLING LOAD

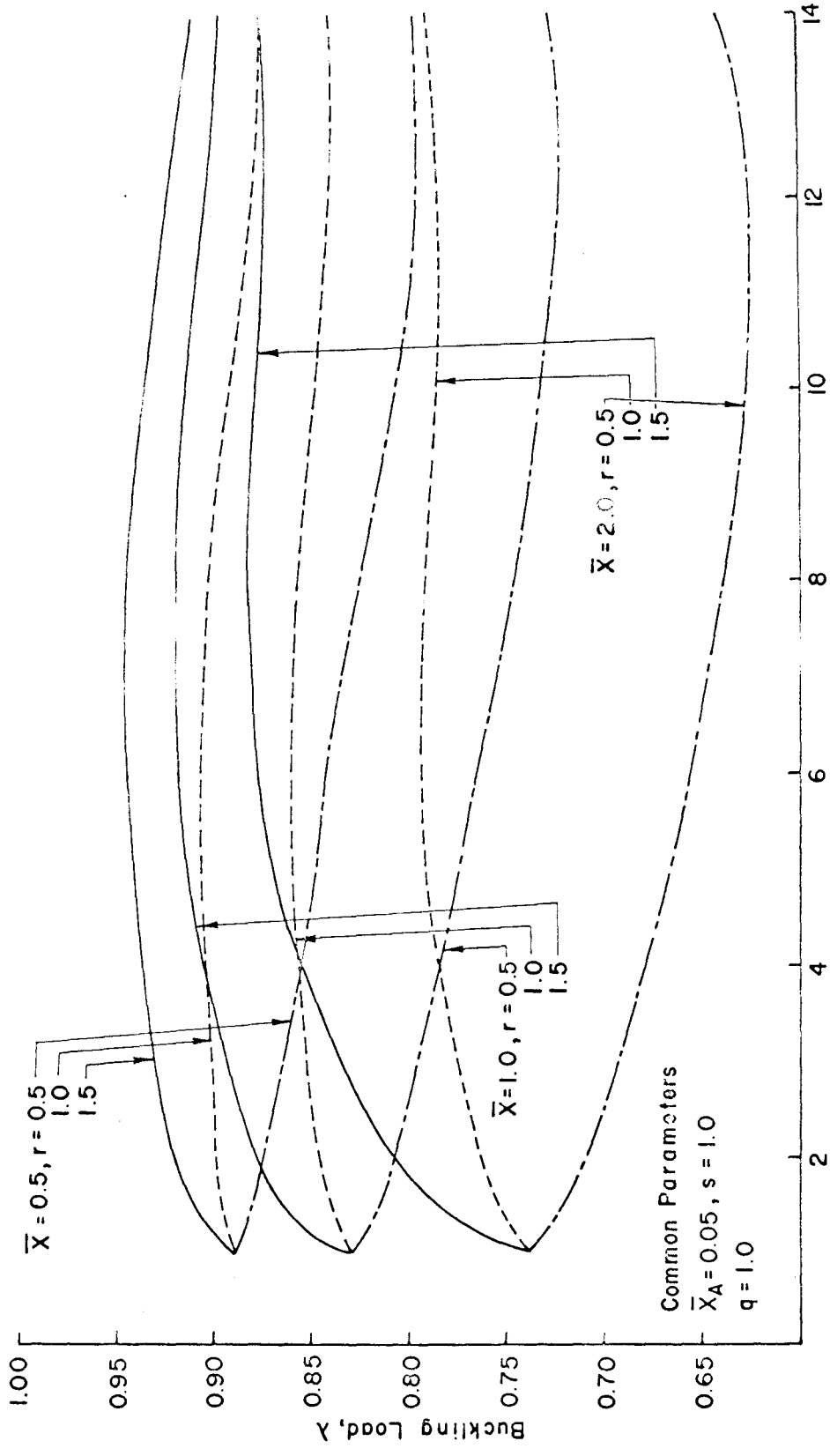

FIG. 21 COMPUTED BUCKLING LOAD

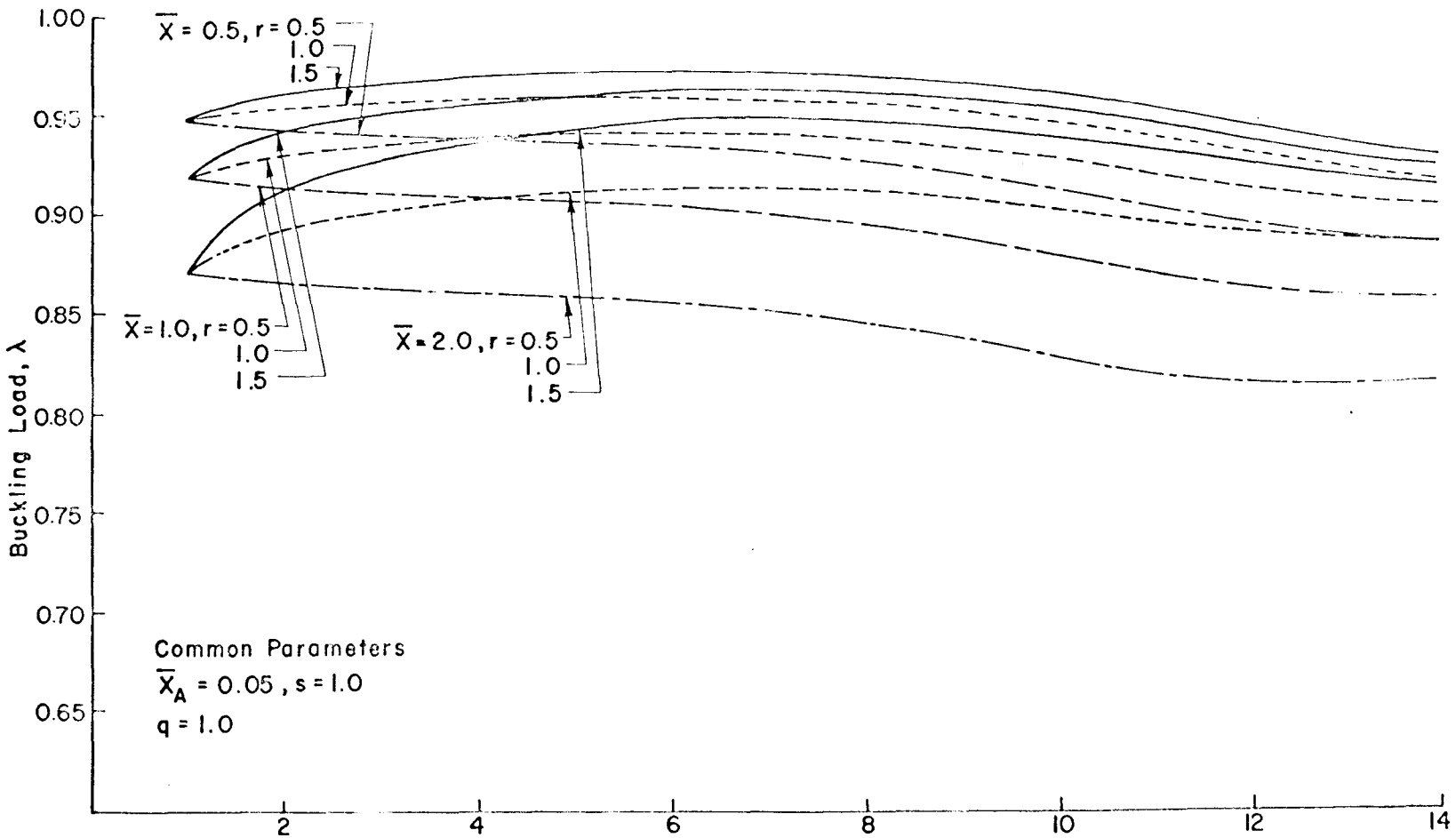

FIG. 22 COMPUTED BUCKLING LOAD

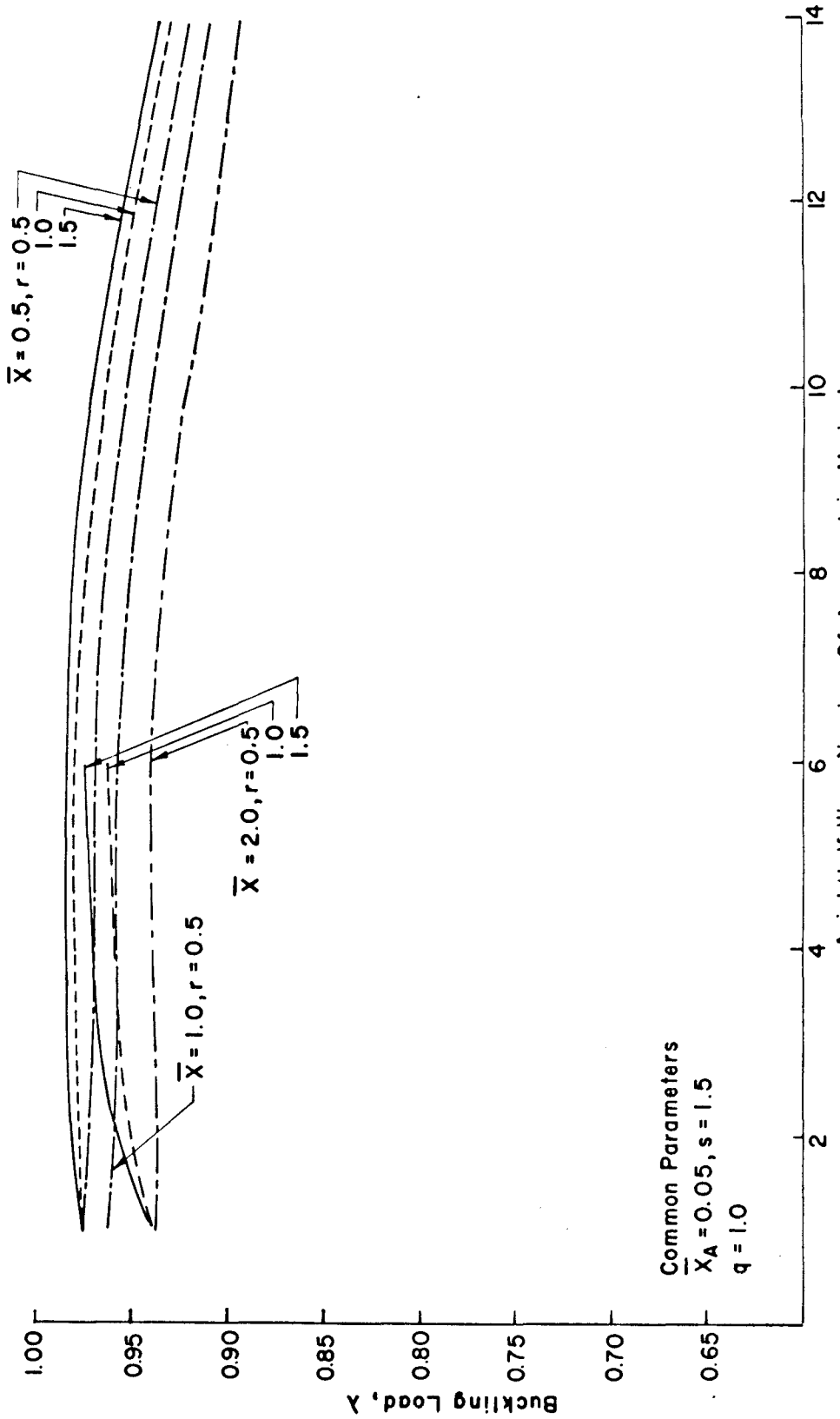

FIG. 23 COMPUTED BUCKLING LOAD

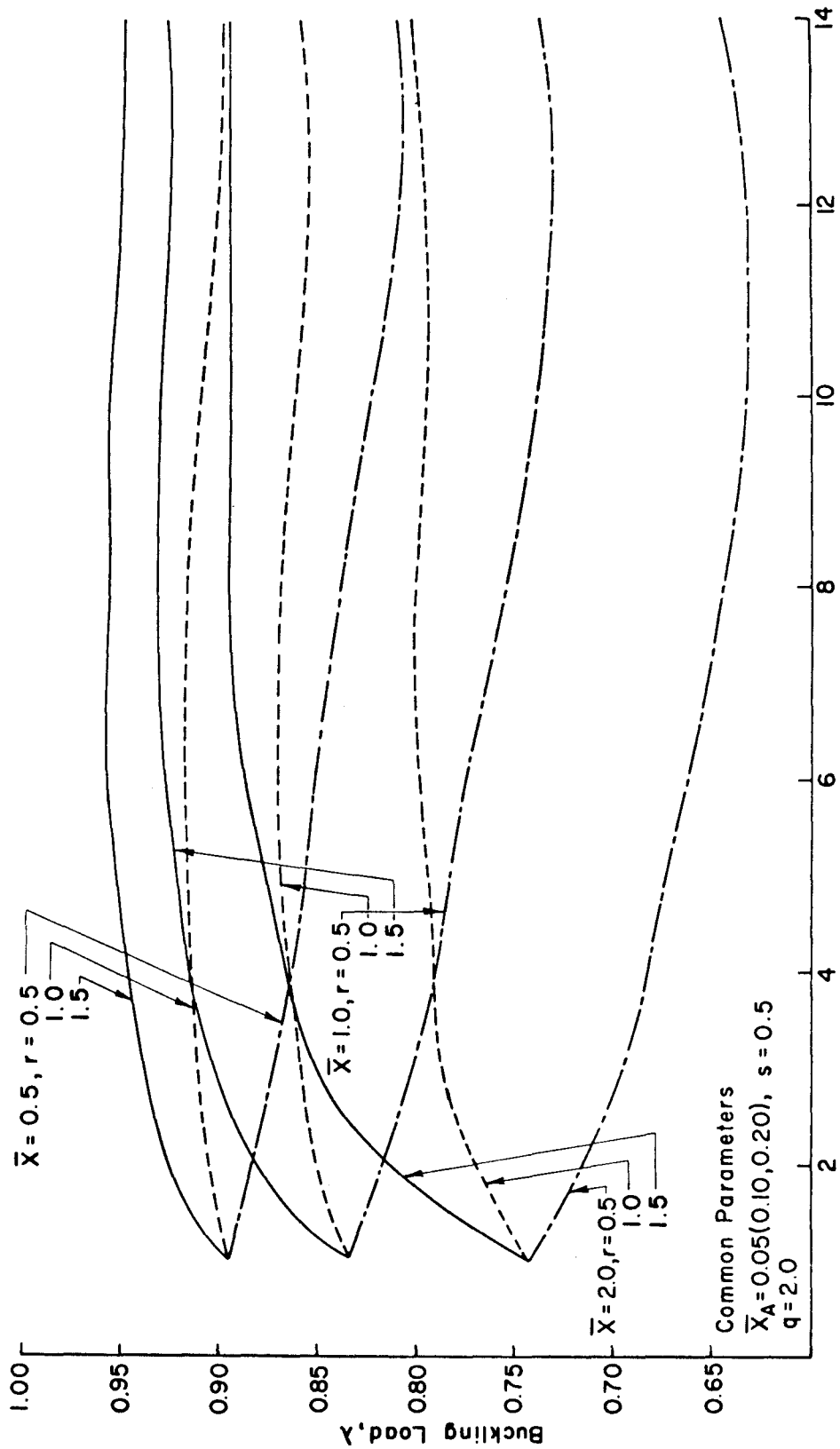

FIG. 24 COMPUTED BUCKLING LOAD

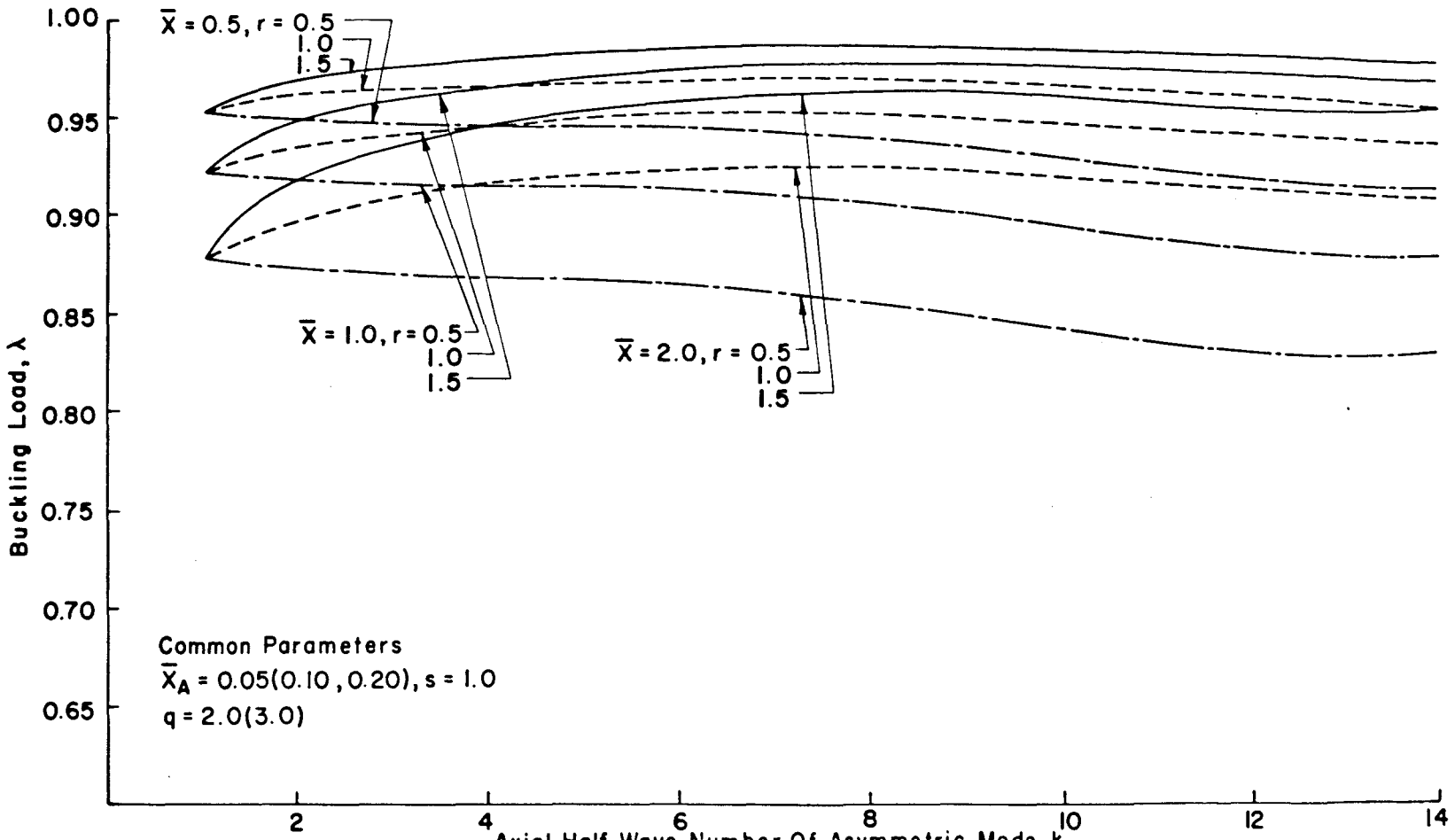

FIG. 25 COMPUTED BUCKLING LOAD

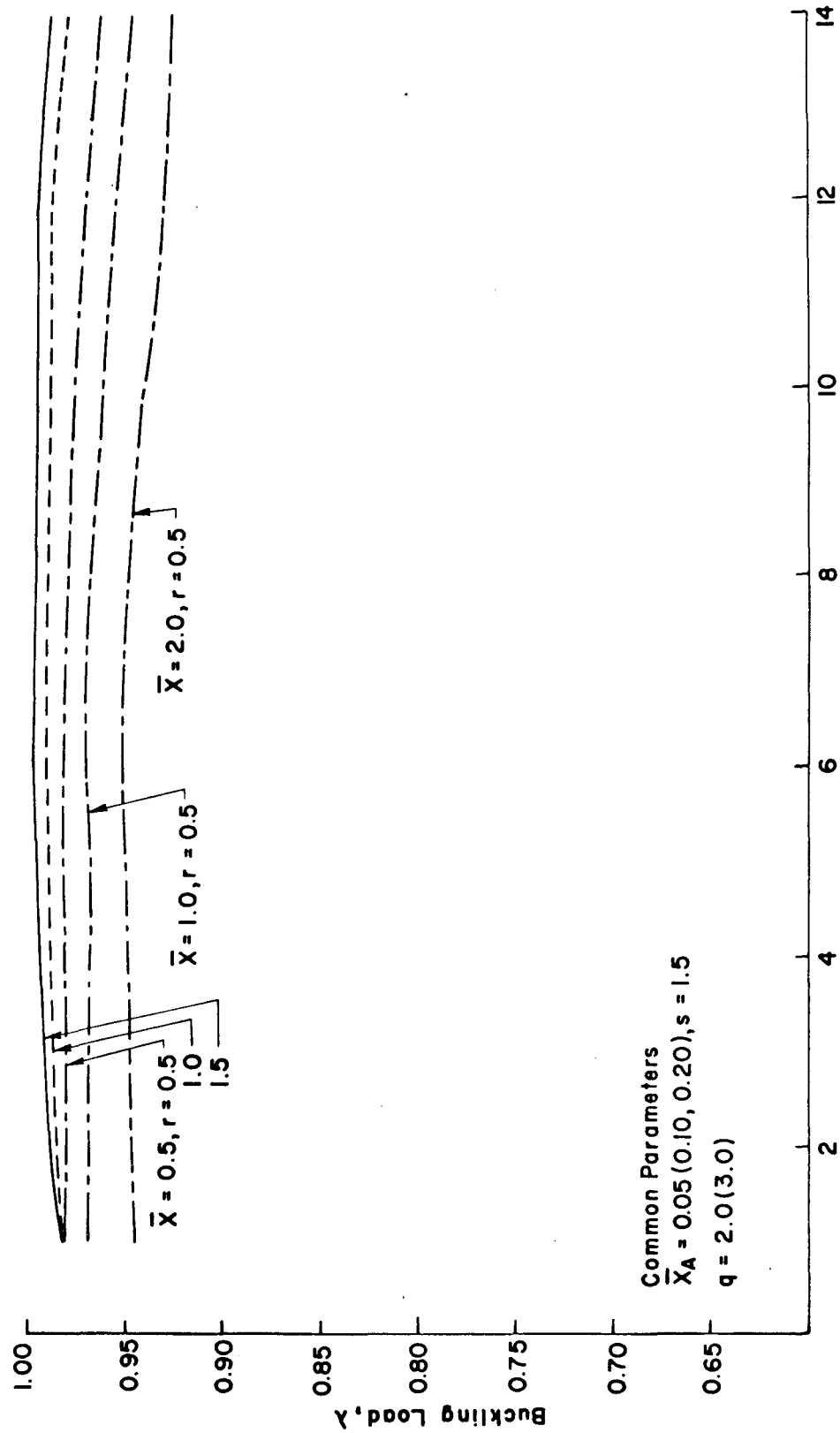

FIG. 26 COMPUTED BUCKLING LOAD

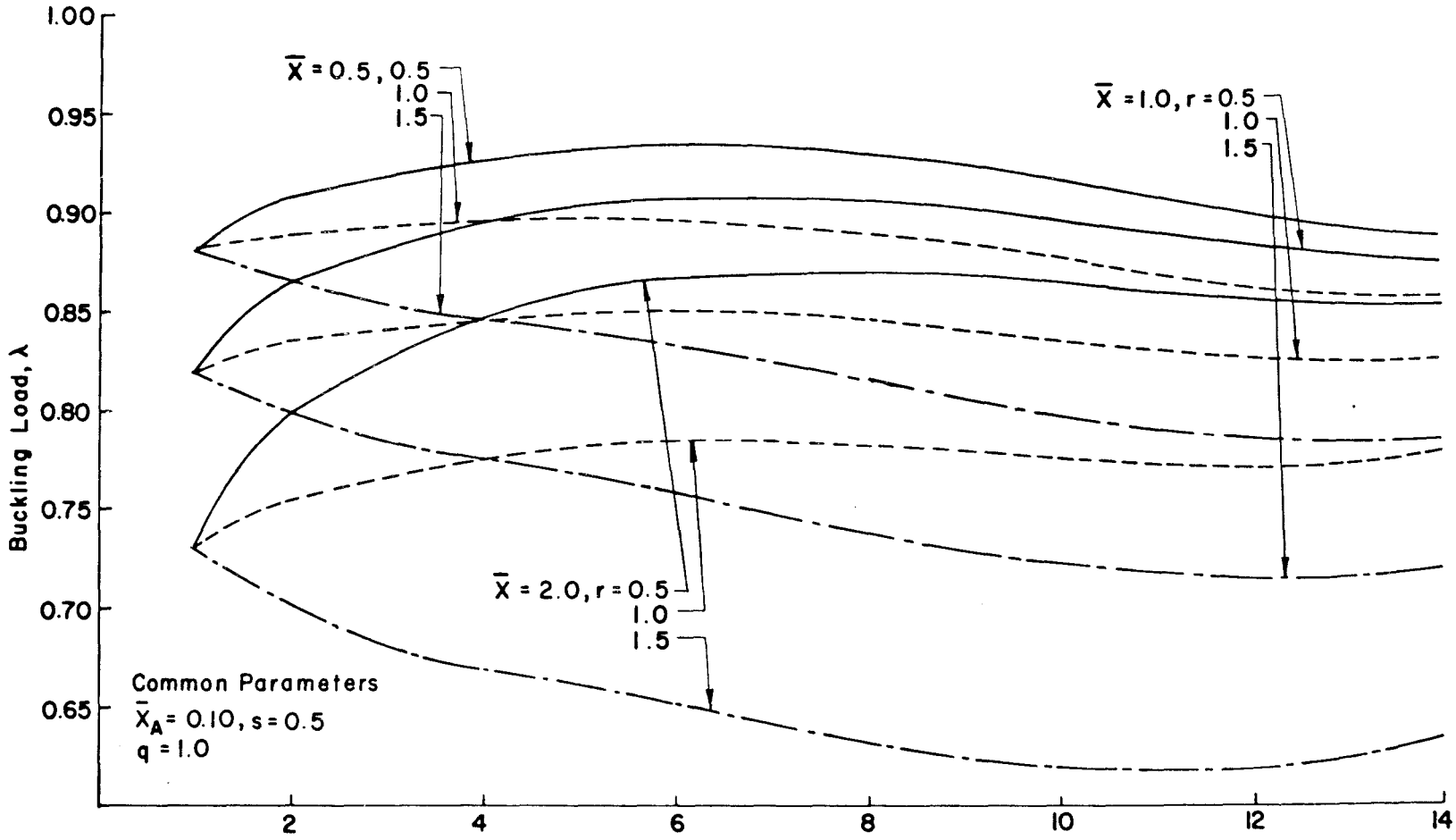

FIG. 27 COMPUTED BUCKLING LOAD

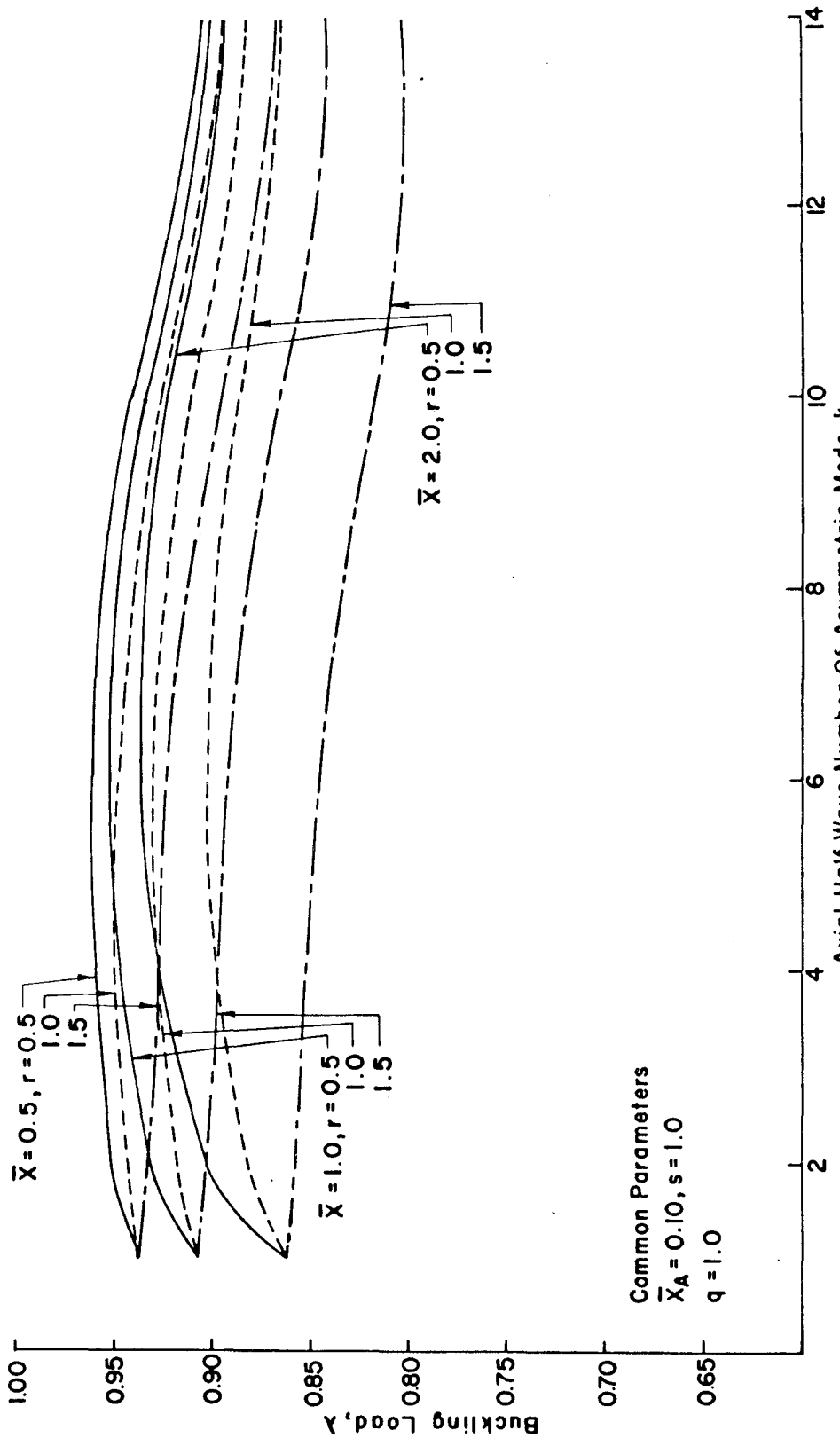

FIG. 28 COMPUTED BUCKLING LOAD

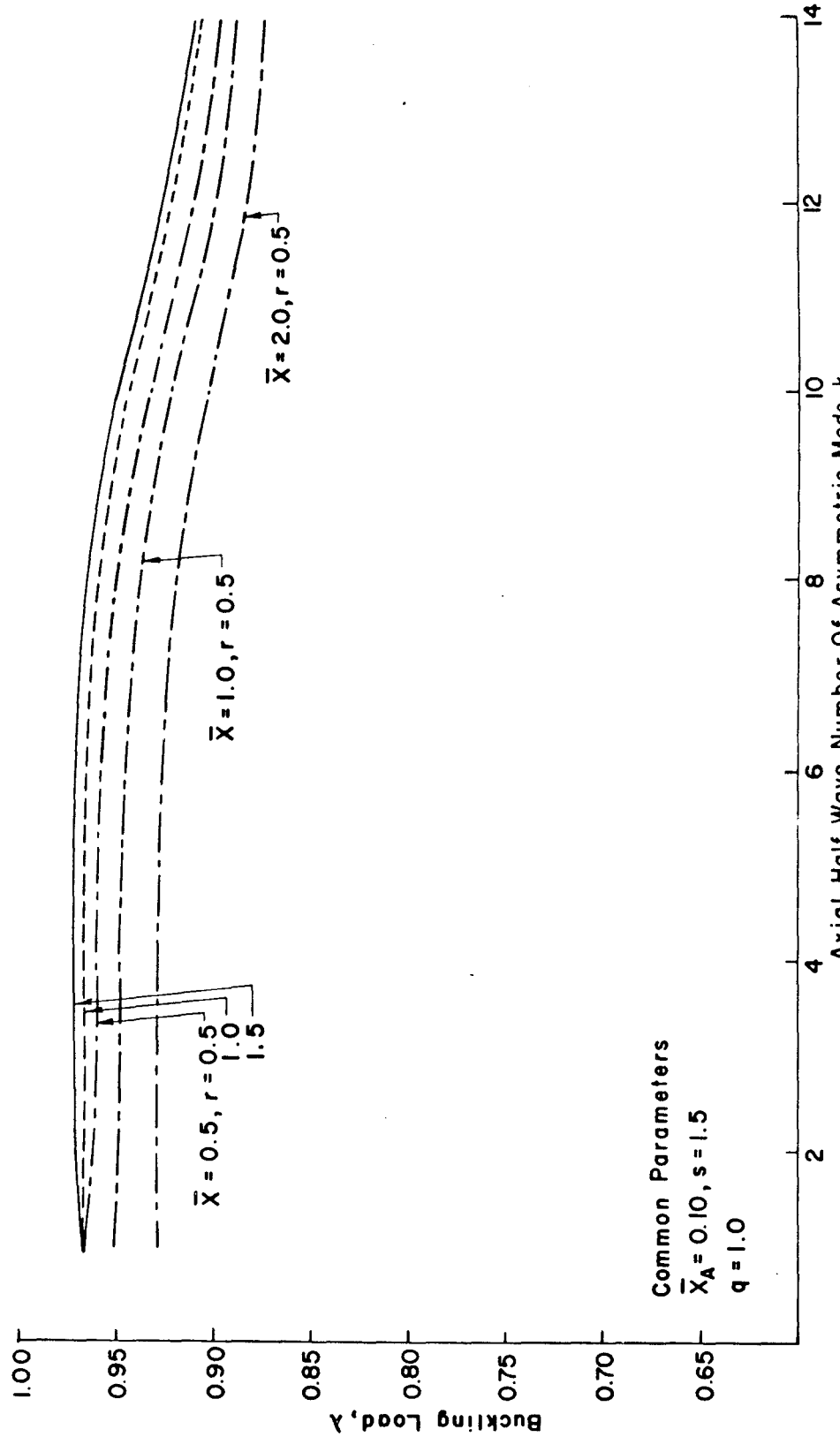

FIG. 29 COMPUTED BUCKLING LOAD

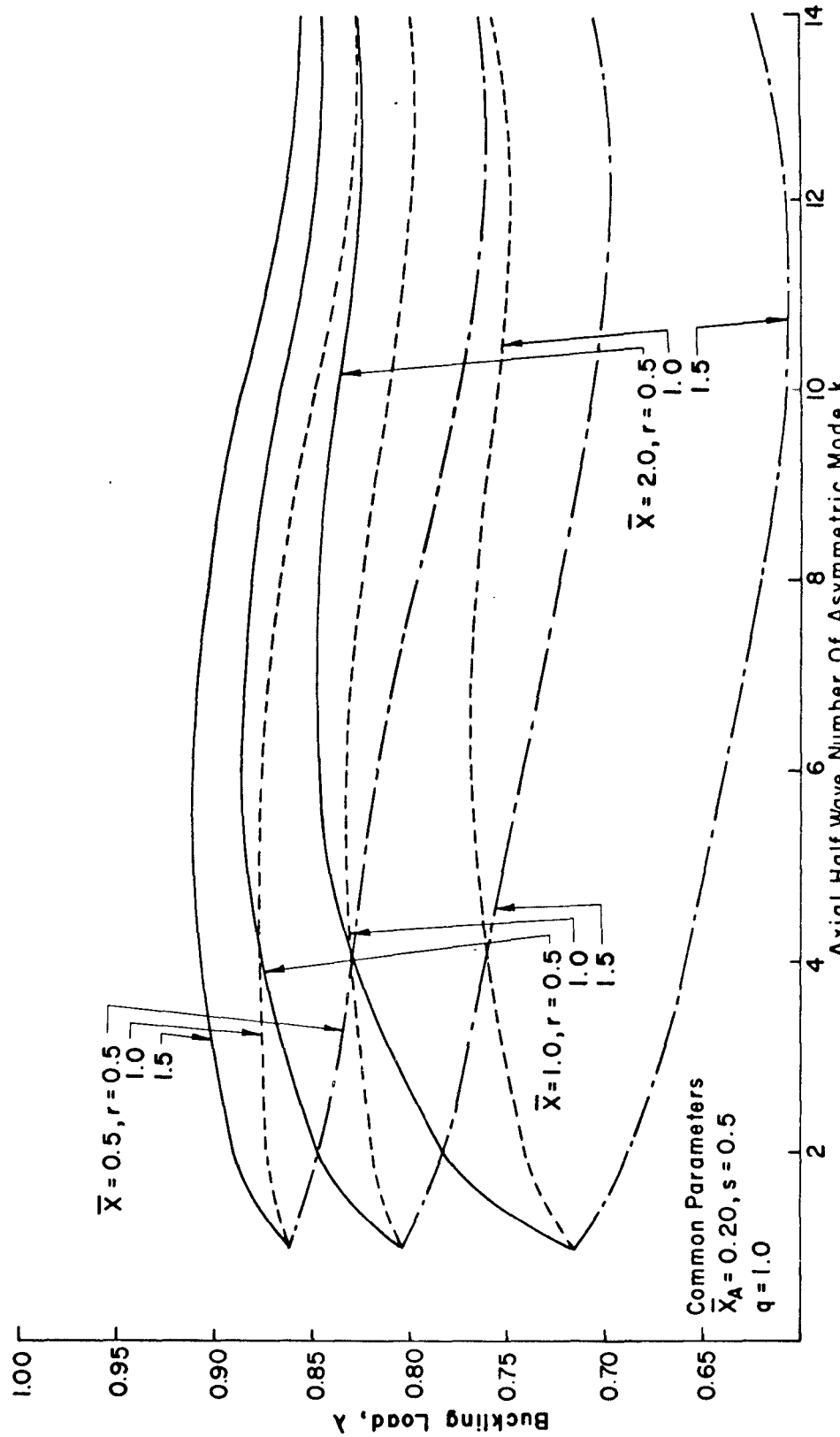

FIG. 30 COMPUTED BUCKLING LOAD

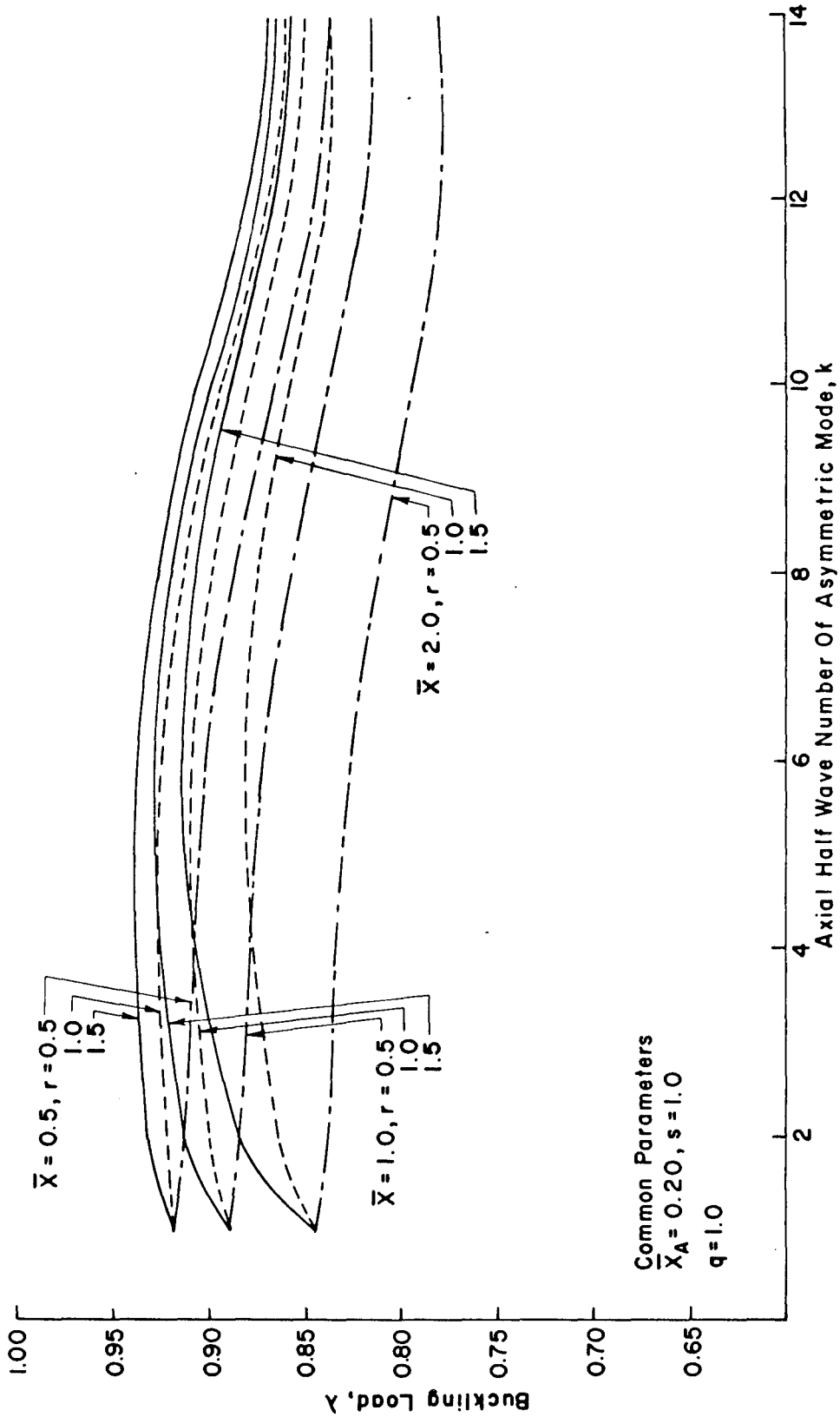

FIG. 31 COMPUTED BUCKLING LOAD

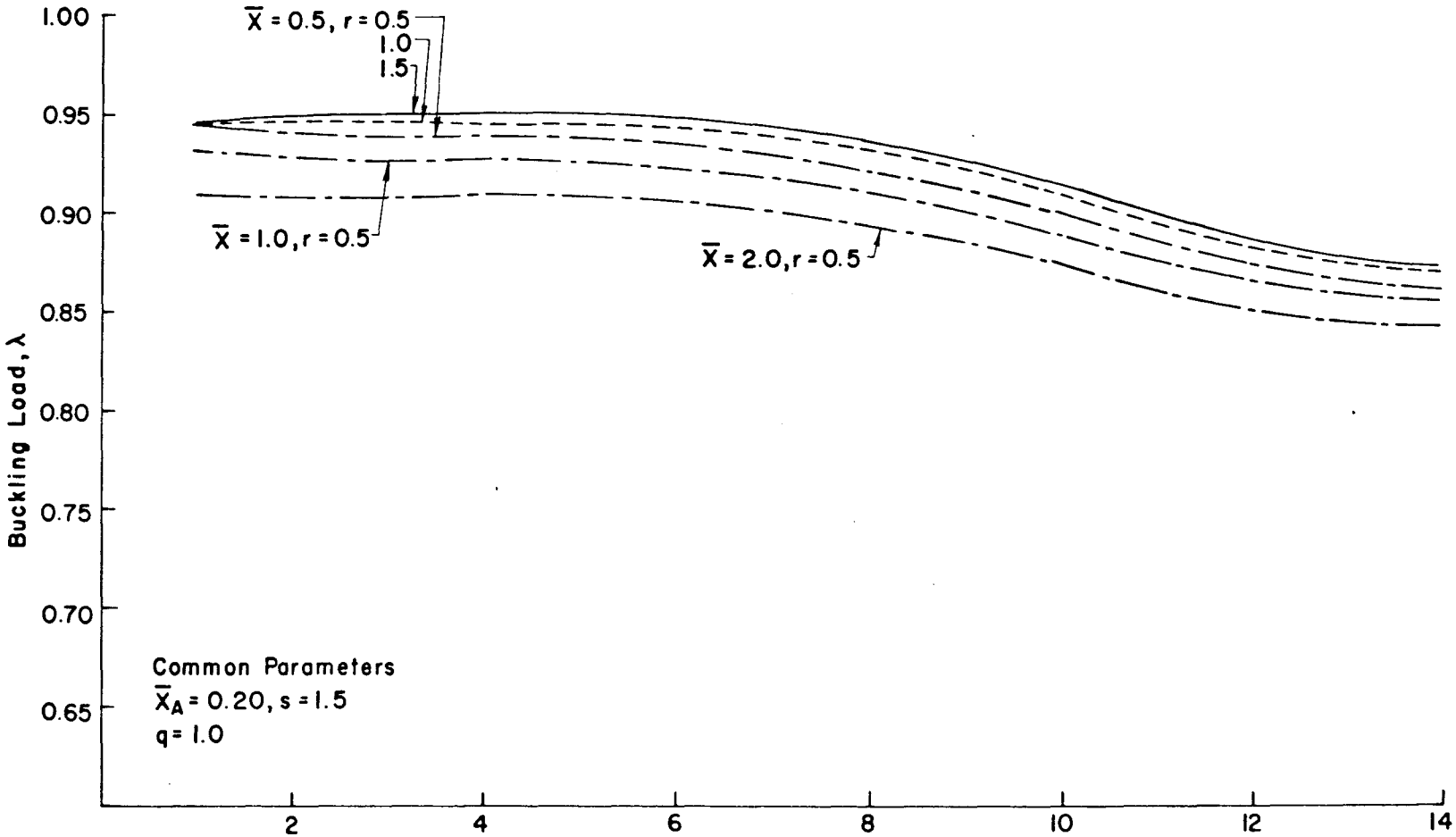

FIG.32 COMPUTED BUCKLING LOAD